



저작자표시-비영리-변경금지 2.0 대한민국

이용자는 아래의 조건을 따르는 경우에 한하여 자유롭게

- 이 저작물을 복제, 배포, 전송, 전시, 공연 및 방송할 수 있습니다.

다음과 같은 조건을 따라야 합니다:



저작자표시. 귀하는 원저작자를 표시하여야 합니다.



비영리. 귀하는 이 저작물을 영리 목적으로 이용할 수 없습니다.



변경금지. 귀하는 이 저작물을 개작, 변형 또는 가공할 수 없습니다.

- 귀하는, 이 저작물의 재이용이나 배포의 경우, 이 저작물에 적용된 이용허락조건을 명확하게 나타내어야 합니다.
- 저작권자로부터 별도의 허가를 받으면 이러한 조건들은 적용되지 않습니다.

저작권법에 따른 이용자의 권리는 위의 내용에 의하여 영향을 받지 않습니다.

이것은 [이용허락규약\(Legal Code\)](#)을 이해하기 쉽게 요약한 것입니다.

[Disclaimer](#)

**A THESIS
FOR THE DEGREE OF MASTER OF SCIENCE**

**Therapeutic effects of *Ishige okamurae* extract and its
constituent Ishophloroglucin A against diabetic-related
angiogenesis**

FERNANDO KURUKULASURIYA HIRUNI NIMASHA

Department of Marine Life Sciences

JEJU NATIONAL UNIVERSITY
REPUBLIC OF KOREA

August, 2019

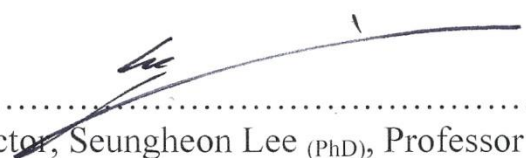
**Therapeutic effects of *Ishige okamurae* extract and its constituent
Ishophloroglucin A against diabetic related angiogenesis**


FERNANDO KURUKULASURIYA HIRUNI NIMASHA
(Supervised by Prof. You-Jin Jeon)

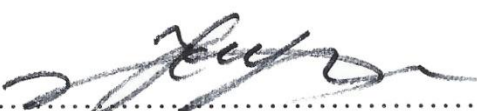
A thesis submitted in partial fulfillment of the requirement for the degree of

MASTER OF SCIENCE
August 2019

The thesis has been examined and approved by


.....
Thesis Director, Seungheon Lee (PhD), Professor of Marine Life sciences,
Jeju National University


.....
Asanka Sanjeewa (PhD), Post Doctorial Researcher of Marine Life sciences,
Jeju National University


.....
You-Jin Jeon (PhD), Professor of Marine Life sciences,
Jeju National University

2019/8
Date

Department of Marine Life Sciences

Graduate School
Jeju National University
Republic of Korea

Table of Contents

Table of contents.....	i
Summary.....	iii
List of Figures.....	v
List of Tables.....	x
Chapter-1, Attenuation of high glucose-induced angiogenesis by <i>Ishige okamurae</i> extract and its constituent Ishophloroglucin A.....	1
Abstract.....	2
1.1. Introduction.....	3
1.2. Materials and Methods.....	6
1.2.1. Materials.....	6
1.2.2. Preparation of IO extract and IPA.....	6
1.2.3. Treatments of IO extract and IPA in zebrafish transgenic (flk:EGFP) embryos.....	7
1.2.4. Zebrafish transgenic (flk:EGFP) embryos and angiogenesis Assays.....	7
1.2.5. Cell culture.....	8
1.2.6. Analysis of glucose concentraion for high glucose-induced angiogenesis.....	8
1.2.7. Analysis of cell viability.....	9
1.2.8. Scratch-wound cell migration Assay.....	9
1.2.9. Tube formation Assay.....	10
1.2.10. In silico docking of VEGFR-2 receptor and IPA.....	10
1.2.11. Western blot Analysis.....	11
1.2.12. Statistical Analysis.....	11
1.3. Results.....	12
1.3.1. Effects of IO extract on high glucose-treated zebrafish embryo.....	12
1.3.2. Effects of IPA on high glucose-treated zebrafish embryo.....	14
1.3.3. Glucose induced angiogenesis in EA.hy926 cells.....	17
1.3.4. Effects of IPA on high glucose-induced cell proliferation, migration, and capillary-like structure formation.....	19
1.3.5. Analysis of molecular docking of IPA and VEGFR-2 Receptor.....	24
1.3.6. Effects of IPA on VEGFR-2 and downstream signaling cascade.....	27
1.4. Discussion.....	29
Conclusion.....	31
References.....	32
Chapter-2, Inhibitory activity of <i>Ishige okamurae</i> extract and its Constituent Ishophloroglucin A against diabetic retinopathy.....	37

Abstract.....	38
2.1. Introduction.....	39
2.2. Materials and Methods.....	41
2.2.1. Cell culture.....	41
2.2.2. Cell treatment with glucose	41
2.2.3. Determination of cytotoxicity of IO extract and IPA in HRMECs	41
2.2.4. Determination of anti-proliferative activity	42
2.2.5. Scratch wound cell migration assay.....	42
2.2.6. Tube formation Assay.....	43
2.2.7. NO inhibition by IPA.....	43
2.2.8. Western blotting.....	44
2.2.9. In vivo inhibition of vascular permeability by IPA	45
2.2.10. Statistical Analysis.....	45
2.3. Results.....	46
2.3.1. Glucose-Induced Angiogenesis in HRME Cells and Cytotoxicity of IO extract and IPA in HRME cells.....	46
2.3.2. IO extract and IPA suppress high glucose-induced cell proliferation	48
2.3.3. IO extract and IPA suppress high glucose-induced cell migration.....	50
2.3.4. IO extract and IPA suppress high glucose-induced capillary formation	53
2.3.5. IPA inhibits NO production in high glucose treated HRME cells.....	56
2.3.6. IPA inhibits vascular permeability in vivo	58
2.4. Discussion.....	60
Conclusion	61
References.....	62
Acknowledgement.....	64

Summary

Diabetes mellitus is associated with secondary metabolic complications, such as insulin resistance and hyperinsulinemia leading to abnormal angiogenesis. Development of new microvessels from the existing vessels is known as angiogenesis. Diabetes is characterized by inadequate angiogenesis in some organs as well as excessive angiogenesis in some others. Apart from its role in several pathological conditions, angiogenesis plays a crucial role in normal growth and development as well. Excessive angiogenesis causes degradation of vascular endothelial cells from the extracellular matrix, enhancement of cell proliferation, migration and formation of extravascular networks. Excessive angiogenesis is also observed in diabetic retinopathy resulting in loss of vision.

Marine algae are considered as a prolific source of important bioactive compounds that aid in maintaining normal health and mitigating disease risks. Among the marine algae, brown algae and its constituent phlorotannins are widely studied for various biological effects by several research groups globally. *Ishige okamurae* (IO) is an edible brown alga found abundantly in the coastal areas of Jeju island. It has been reported that IO exerts several biological activities, such as anti- α -glucosidase, free-radical scavenging, cytoprotective, anti-obesity, and anti-inflammatory activities. Ishophloroglucin A (IPA) is a novel phlorotannin isolated from IO extract which has been studied for standardizing the anti- α -glucosidase activity of IO. However, IO extract and IPA have not been examined for diabetic-related pathologies. Therefore, in the present study, IO extract and IPA were studied for their anti-angiogenic effects on high glucose-induced vascular growth.

Zebrafish model is widely used in studies on angiogenesis. Transgenic zebrafish lines are more convenient for imaging of the vessels due to fluorescent labeling. In this study, transgenic zebrafish Tg(*flk:EGFP*), was used to evaluate the anti-angiogenesis effects. The vascular endothelium is a biologically important layer present in the blood vessels and its

dysfunction results in various vascular pathologies. The EA.hy926 cell line is frequently used in different angiogenesis studies. These cells are more convenient than primary vascular cells because they are mortal and do not possess variations associated with the donor. In this study, the anti-angiogenic effects of IPA were evaluated in EA.hy926 cells. IPA treatment decreased cell proliferation, cell migration, and capillary-like structure formation in high glucose-treated EA.hy926 cells. In silico stimulations revealed that IPA binds to the active site of VEGFR-2 (PDB ID: 2OH4) with a binding energy of -656.948 kcal/mol. IPA treatment down regulated vascular endothelial growth factor receptor 2 (VEGFR-2) expression and its downstream signaling molecules.

As the chapter 1, the attenuation of high glucose-induced angiogenesis by *Ishige okamurae* extract and its constituent Ishophloroglucin A was discussed. Furthermore, the effects of IPA was studied for diabetes retinopathy in high glucose-treated human retinal microvascular endothelial cells (HRMEC) in the chapter 2 of the study. The results showed that IPA treatment suppressed the angiogenesis in retinal endothelial cells by down regulating the vascular permeability in vitro and in vivo. Overall, these findings suggest that IO extract and IPA are potential agents for the development of therapeutics against diabetes-related angiogenesis.

Key Words: Angiogenesis; Diabetes; *Ishige okamurae*; Ishophloroglucin A

List of figures

Part 1

Figure 1-1. Structure of Ishophloroglucin A (IPA) isolated from *Ishige okamurae*.....5

Figure 1-2. Effects of *Ishige okamurae* (IO) extract on zebrafish embryo. (A) Effects of IO extract on the survival rate of transgenic zebrafish (*flk:EGFP*) embryos. The embryos were treated with 10, 30, and 100 µg/mL of IO extract for 24, 48, 72, 96, 120, 144, and 168 hours post fertilization (hpf). The treatment effects were normalized to blank (0 µg/mL IO extract). (B) Fluorescence microscopic images of the retinal vessels of transgenic zebrafish (*flk:EGFP*) embryos treated with IO extract. (C) The diameter of the hyaloid retinal vessel treated with IO extract. (D) Images of the whole body vessel formation in transgenic zebrafish (*flk:EGFP*) embryos treated with IO extract as obtained by fluorescence microscopy. (E) Quantified fluorescence intensity of the whole body treated with IO extract (a: 0 mM glucose + 0 µg/mL IO, b: 130 mM glucose + 0 µg/mL IO, and c: 130 mM glucose + 10 µg/mL IO). The effects of 130 mM glucose on vessel formation were compared with B [blank (0 mM glucose + 0 µg/mL IO extract)]. The effects of IPA on high glucose-induced vessel formation were normalized to C [control (130 mM glucose + 0 µg/mL IO extract)].....13

Figure 1- 3. Effects of IPA on transgenic zebrafish (*flk:EGFP*) embryos. (A) Effects of IPA on the survival rate of transgenic zebrafish (*flk:EGFP*) embryos. The embryos were treated with 0.3, 1.5, 3, and 5 µM IPA for 24, 48, 72, 96, 120, 144, and 168 hpf. The treatment effects were normalized to blank (0 µM IPA). (B) Fluorescence microscopic images of the retinal vessels of transgenic zebrafish (*flk:EGFP*) embryos treated with IPA. (C) The diameter of hyaloid retinal vessels treated with IPA. (D) The images of whole body vessel formation in transgenic zebrafish (*flk:EGFP*) embryos treated with IPA as obtained by

fluorescence microscopy. (E) Quantified fluorescence intensity of the whole body treated with IO extract (a: 0 mM glucose + 0 μ M IPA, b: 130 mM glucose + 0 μ M IPA, c: 130 mM glucose + 0.015 μ M IPA, d: 130 mM glucose + 0.05 μ M IPA, e: 130 mM glucose + 0.15 μ M IPA, and f: 130 mM glucose + 0.5 μ M IPA). The effects of 130 mM glucose on vessel formation were compared to B [blank (0 mM glucose + 0 μ M IPA)]. The effects of IPA on high glucose-induced vessel formation were normalized to C [control (130 mM glucose + 0 μ M IPA)].....15,16

Figure 1-4. Effect of glucose on the proliferation of vascular endothelial cell Ea.hy926. (A) Cell viability upon treatment with glucose for 24 h. Cells were incubated with increasing concentrations of glucose (zero mM, five mM, 10 mM, 30 mM, 50 mM, and 100 mM) for 24 h, and cell viability was determined by the MTT assay. Results are normalized to blank (0 mM of glucose). Cell viability upon the treatment with 30 mM of glucose for 24 h was assessed using the Muse™ Count and Viability Kit; representative viability profiles (dot plots) (B) and viable cell count are shown (C). The results were obtained using Muse™ Cell Analyzer.....18

Figure 1-5. IPA inhibits the proliferation of EA.hy926 cells. (A) Cytotoxicity of IPA in EA.hy926 cells. The cells were treated with different IPA concentrations (0, 0.05, 0.15, 0.5, 1.5, and 2.5 μ M) for 24 h and the cell viability was determined by MTT assay. The results were normalized to blank (0 μ M IPA). (B) IPA inhibits the proliferation of high glucose-induced EA.hy926 cells. The cells were treated with different concentrations of IPA (0.05, 0.15, 0.5, and 1.5 μ M) along with 30 mM glucose. MTT assay was performed to determine cell viability. The anti-proliferative effects of IPA in high glucose-induced cells were normalized to C [control (30 mM glucose + 0 μ M IPA)] and the effects of 30 mM glucose were compared to B [blank (0 mM glucose + 0 μ M IPA)].....21

Figure 1-6. (A) IPA inhibits high glucose-induced cell migration. The cells were treated with different concentrations of IPA (0.15, 0.5, and 1.5 μ M) along with 30 mM glucose. The cell monolayer was scraped at the middle of the well and the initial gap length (0 h) and the final gap length (12 h) was measured. (B) The gap closure was quantified by percentage (%). The effects of 30 mM glucose on cell migration were compared to B [blank (0 mM glucose + 0 μ M IPA)], The effects of IPA on high glucose-induced cell migration were normalized to C [control (30 mM glucose + 0 μ M IPA)].....22

Figure 1-7. (A) IPA suppresses high glucose-induced capillary formation in Matrigel®. The cells were seeded on Matrigel® with different concentrations of IPA (0.15, 0.5, and 1.5 μ M) along with 30 mM glucose including B [blank (0 mM glucose + 0 μ M IPA)] and C [control (30 mM glucose + 0 μ M IPA)]. After 6 h incubation, the cells were photographed and the angiogenic score was determined. (B) Quantification of capillary formation. The effects of 30 mM glucose on capillary formation were compared to B [blank (0 mM glucose + 0 μ M IPA)]. The effects of IPA on high glucose-induced capillary formation were normalized to C [control (30 mM glucose + 0 μ M IPA)].....23

Figure 1-8. Computational prediction of the VEGFR-2 receptor and docking simulation with IPA.....26

Figure 1-9. (A) IPA inhibits VEGFR-2 and its downstream signaling molecules. IPA attenuating high glucose-induced phosphorylation of VEGFR-2 and downstream signaling molecules ERK, AKT, JNK, and eNOS were detected using western blotting. (B) Quantitative evaluation of the protein expression. The effects of 30 mM glucose on the expression of each protein were compared to B [blank (0 mM glucose + 0 μ M IPA)]. The effects of IPA on high glucose-induced protein expression were normalized to C [control (30 mM glucose + 0 μ M IPA)].....28

Part 2

Figure 2-1. (A) HRME Cell viability upon treatment with glucose for 24 h. (B) IO cytotoxicity for HRME cells (C) IPA Cytotoxicity for HRME cells. Cells were incubated with increasing concentrations of glucose (25 mM, 30 mM, 50 mM, and 100 mM), IO extract (3 µg/ml, 10 µg/ml, 30 µg/ml, 50 µg/ml, 100 µg/ml, 150 µg/ml), IPA (0 µM, 0.15 µM, 0.5 µM, 1.5 µM, 5 µM, and 15 µM) for 24 h, and cell viability was determined by the MTT assay. Results are normalized to blank (No treatment).....47

Figure 2-2. (A) Antiproliferation effect of IO extract (B). Antiproliferation effect of IPA. Cells were treated without glucose or sample (B, blank), with 30 mM of glucose without sample (C, control) and with different concentrations of IO (30 µg/ml, 50 µg/ml, 100 µg/ml, 150 µg/ml) or IPA (0.15 µM, 0.5 µM, 1.5 µM) together with 30 mM of glucose. Cells were incubated for 24 h and cell viability was measured by MTT assay. Effect of 30 mM of glucose on cell proliferation is compared with B; blank, Anti-proliferation effect of samples in high glucose-treated cells is normalized to C; control.....49

Figure 2-3. (A) IO extract inhibited the migration of EA.hy926 cells treated with high glucose concentrations. (B) Quantitative evaluation of migration inhibition of IO extract in high glucose-induced EA.hy926 cells. (C) IPA inhibited the migration of EA.hy926 cells treated with high glucose concentrations. (D) Quantitative evaluation of migration inhibition of IPA in high glucose-induced EA.hy926 cells. Cells were treated without glucose or sample (B, blank), with 30 mM of glucose without sample (C, control) and with different concentrations of IO (30 µg/ml, 50 µg/ml, 100 µg/ml, 150 µg/ml) or IPA (0.15 µM, 0.5 µM, 1.5 µM) together with 30 mM of glucose.....51,52

Figure 2-4. (A) IO extract inhibited the capillary formation of EA.hy926 cells treated with high glucose concentrations. (B) Quantitative evaluation of capillary formation inhibition

of IO extract in high glucose-induced EA.hy926 cells. (C) IPA inhibited the capillary formation of EA.hy926 cells treated with high glucose concentrations. (D) Quantitative evaluation of capillary formation inhibition of IPA in high glucose-induced EA.hy926 cells. Cells were treated without glucose or sample (B, blank), with 30 mM of glucose without sample (C, control) and with different concentrations of IO (30 µg/ml, 50 µg/ml, 100 µg/ml, 150 µg/ml) or IPA (0.15 µM, 0.5 µM, 1.5 µM) together with 30 mM of glucose.....54,55

Figure 2-5. (A) IPA inhibition of NO measured by Griess assay. (B) IPA inhibition of NO measured by DAF FM DA assay (C) IPA inhibits eNOs (D) quantitative evaluation of NO inhibition.....57

Figure 2-6. (A) IPA inhibits vascular permeability and vascular leakage in vivo. (B) Vascular leakage quantification upon the treatment of IPA against hypoxia condition (C) Quantification of vessel growth upon the treatment of IPA against hypoxia condition. (a: 0 CoCl₂ mM + 0 µM IPA, b: CoCl₂ mM + 0 µM IPA, c: CoCl₂ mM + 0.015 µM IPA, d: CoCl₂ mM + 0.05 µM IPA, e: CoCl₂ mM + 0.15 µM IPA, and f: CoCl₂ mM + 0.5 µM IPA).....59

List of Tables.

Table 1. Ligands; IPA, Benzimidazole-urea.....25

Table2. The calculated affinities for VEGFR-2.....25

Chapter-1

Attenuation of high glucose-induced angiogenesis by *Ishige okamurae* extract and its constituent Ishophloroglucin A

Abstract

Background: Diabetes is associated with vascular complications, such as impaired wound healing and accelerated vascular growth. The different clinical manifestations, such as retinopathy and nephropathy reveal the severity of enhanced vascular growth known as angiogenesis. This study was performed to evaluate the effects of an extract of *Ishige okamurae* (IO) and its constituent Ishophloroglucin A (IPA) on high glucose-induced angiogenesis.

Methodology: A transgenic zebrafish (*flk:EGFP*) embryo model was treated with IO extract and IPA to evaluate the vessel growth against high glucose-induced angiogenesis. High glucose-induced vascular endothelial, EA.hy926 cells were examined for anti-angiogenesis potential of IPA in cell proliferation, cell migration and capillary formation. The expression of vascular endothelial growth factor receptor 2 (VEGFR-2) and target molecules were assayed by western blotting and the inhibition of the receptor was determined by in silico analysis.

Results: IO extract and IPA suppressed the vessel formation in transgenic zebrafish (*flk:EGFP*) embryo. IPA attenuated cell proliferation, cell migration and capillary-like structure formation in high glucose-treated human vascular endothelial cells. IPA down-regulated the expression of high glucose-induced VEGFR-2 and downstream signaling molecules cascade.

Conclusion: The IO extract and IPA exhibited anti-angiogenic effects against high glucose-induced angiogenesis suggesting their potential for use as therapeutic agents in diabetes-related angiogenesis.

1.1. Introduction

Angiogenesis is the formation of new capillary blood vessels from existing blood vessels, and is distinct from the normal vasculogenesis of blood vessels' formation from precursor cells [1]. Apart from its role in pathologies, angiogenesis is a vitally important process in normal growth including reproduction, development, and repair [2]. In diabetes, a high plasma glucose level causes abnormalities of angiogenesis resulting in vascular dysfunction and serious pathologies [3]. From the vascular point of view, diabetes is known as a “paradoxal disease” due to its dual role in excessive angiogenesis and insufficient angiogenesis in different organs [4]. Enhanced angiogenesis causes diabetic retinopathy [5] and nephropathy [6].

Although abnormal vascular growth is alleviated with antiangiogenic agents, they cause unexpected side effects including endothelial dysfunction and vessel pruning [7]. Therefore, there is a clear need for safer and more effective approaches. Recently, the screening of angiogenesis inhibitors from phytonutrients and dietary bioactives has taken much attention due to their low cost and relative safety [8]. Indeed, it was shown that marine algae-derived fucoxanthin [9] and bromophenols [8] serve as angiogenesis inhibitors.

Ishige okamure (IO) is an edible brown alga grown in the subtidal regions of Jeju island, South Korea [10]. It has been reported that IO exerts several biological activities, such as anti- α -glucosidase, free-radical scavenging, cytoprotective, anti-obesity, and anti-inflammatory activities [11-13] Ishophloroglucin A (IPA) is a novel phlorotannin isolated from IO extract which has been studied for standardizing the anti- α -glucosidase activity of IO [14]. However, no research has been carried out to assess the protective effect of IO extract and IPA against angiogenesis resulting from high glucose levels. Therefore, in the present study, we evaluated the antiangiogenesis activity of IO extract and IPA against high glucose-induced angiogenesis in vitro and in vivo models. Hence, the vascular endothelial

cell EA.hy926 was used in the present study to investigate the inhibitory effects of IPA against high glucose-induced angiogenesis. EA.hy926 is a hybrid cell obtained by the fusion of human umbilical vein endothelial cell (HUVEC) with the human lung carcinoma cell line A549. EA.hy926 cells show characteristics of the human vascular endothelium, and its functional stability through passages, which makes it an ideal cell line for angiogenesis-related studies [15-16]. Even though the angiogenesis assays generally utilize the HUVEC isolated from the human umbilical vein, this cell shows several constraints, including limited replication potential and distinct characteristics of primary source material [17]. Therefore, compared to HUVEC, EA.hy926 cells are known to be a homogeneous experimental model assuring the reproducibility of the data [18]. The anti-angiogenesis activity of IPA in EA.hy926 cells was investigated by assessing cell proliferation, migration, and tube formation, which are known as key steps in angiogenesis. The inhibition of vascular endothelial growth factor receptor 2 (VEGFR-2) is a major approach in anti-angiogenic drug development [19]. IPA inhibition of VEGFR-2 was determined by *in silico* analysis. The expression levels of VEGFR-2 and several downstream signaling molecules were examined to elucidate the mechanism of action of IPA against high glucose-induced angiogenesis. Furthermore, the effect of IPA against high glucose-induced angiogenesis was evaluated *in vivo* model using zebrafish embryos.

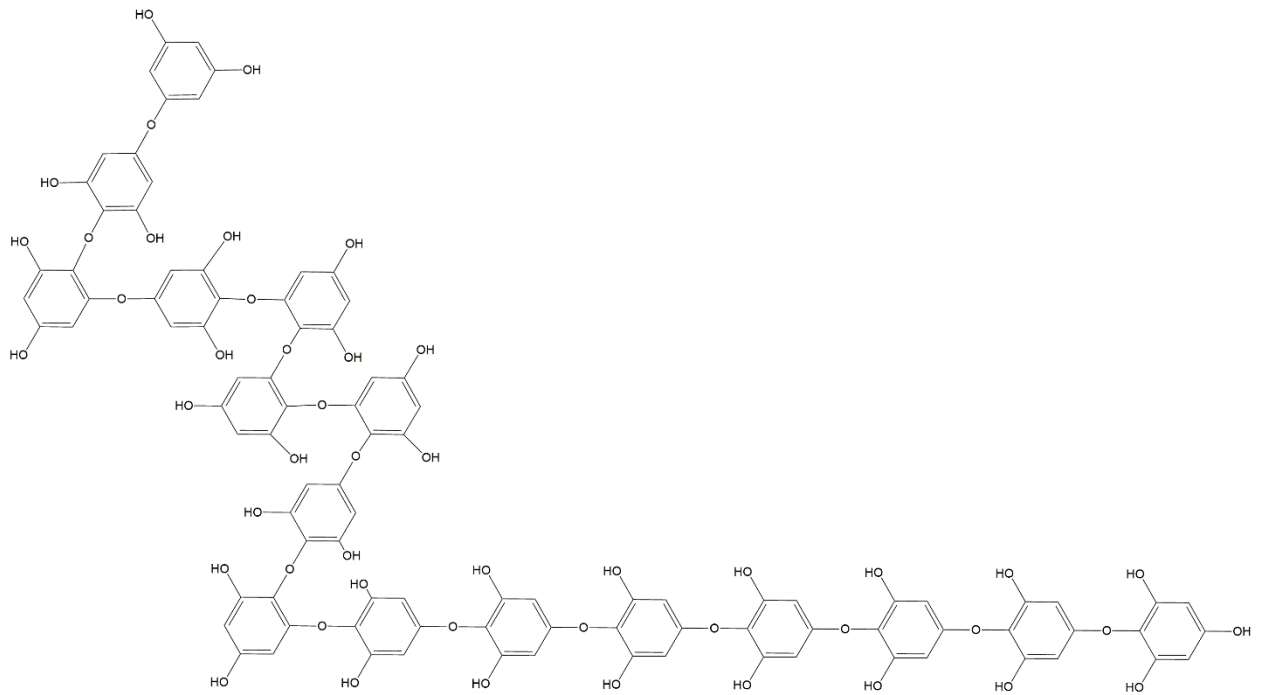


Figure 1-1.Structure of Ishophloroglucin A (IPA) isolated from *Ishige okamurae*

1.2. Materials and Methods

1.2.1. Materials

The human vascular endothelial cell line, EA.hy926 was obtained from the American Type Culture Collection (ATCC, Rockville, MD, USA). Dulbecco's Modified Eagle Medium (DMEM) and penicillin, streptomycin mixture were purchased from Gibco Life Technologies, Grand Island, NY, USA. Fetal Bovine Serum (FBS) was purchased from Merck, Sacramento, CA, USA. 3-(4, 5-dimethylthiazol-2-yl)-2, 5-diphenyltetrazolium bromide (MTT) was obtained from VWR Life Science (Lutterworth, UK). Dimethyl sulfoxide (DMSO) was purchased from Amresco, Life Sciences, OH, Solon, USA. Matrigel® was obtained from BD Biosciences, Bedford, MA, USA. Both primary and secondary antibodies used in Western blot analysis were purchased from Santa Cruz Biotechnology (Santa Cruz, CA, USA). All other chemicals were commercially available analytical grade.

1.2.2. Preparation of IO extract and IPA

Ishige okamurae was collected in April 2016 in Seongsan in Jeju Island, South Korea. Preparation of IO extract and isolation of IPA were carried out according to the previously described method [14]. Briefly, 50% ethanolic extract of IO was fractionated through centrifugal partition chromatography (CPC 240, Tokyo, Japan) and further purified by semipreparative HPLC column (YMC-Pack ODS-A, 10×250 mm, 5µm) to obtain IPA. The identity of IPA (99% of purity) was verified by MS fragmentation of m/z 1986.26 at an ultrahigh resolution Q-TOF LC-MS/MS coupled with an electrospray ionization (ESI) resource (maXis-HD, Bruker Daltonics, Bremen, Germany) at Korea Basic Science

Institute (KBSI) in Ochang, South Korea. According to the validated method of previous study [14], IO extract in this study have 1.8 % of IPA.

1.2.3. Treatments of IO extract and IPA in zebrafish transgenic (*flk:EGFP*) embryos

Prior to assess the anti-angiogenesis effect, the survival rate upon the treatment of IO extract and IPA were determined in zebrafish transgenic (*flk:EGFP*) embryos. The embryos were kept in 24-well plates and maintained in embryonic water containing different concentrations of IO extract (10, 30, 100 $\mu\text{g/ml}$) or IPA (0.3, 1.5, 3, 5 μM) and survival rates were analyzed for 168 hours post fertilization (hpf).

1.2.4. Zebrafish transgenic (*flk:EGFP*) embryos and angiogenesis Assays

High glucose-induced angiogenesis was developed in zebrafish embryo as described previously [20]. The angiogenesis was induced by maintaining zebrafish transgenic (*flk:EGFP*) embryos [3 days post fertilization (dpf)] in embryonic water containing 130 mM glucose for 3 days. High glucose treated embryos were treated with 10 $\mu\text{g/ml}$ of IO extract or different concentrations of IPA (0.015, 0.05, 0.15, 0.5 μM) and the vessel growth was examined in hyaloid retinal vessels and whole body. The images were taken after 3h of treatment using the fluorescence microscope (LIONHEART^{FX} automated live cell imager). The vessel formation in retinal vessels were evaluated measuring the retinal vessel diameter of the images (10 \times magnification) at 5 different places using Gen5 3.04 software and averaged. The vessel formation of the whole body was assessed by measuring the fluorescence intensities of the images (4 \times magnification) using Image J software.

1.2.5. Cell culture

The human vascular endothelial cell line, EA.hy926 was cultured in DMEM containing 10% FBS and 1% penicillin, streptomycin mixture. Cells were maintained in an atmosphere of 5% CO₂ at 37 °C and plates were split 1:3 when they reached confluence.

1.2.6. Analysis of glucose concentration for high glucose-induced angiogenesis

EA.hy926 cells were plated onto a 96-well plate with three replicates for each concentration. Following 24 h of incubation at 37 °C, different concentrations (0 mM, 5 mM, 10 mM, 30 mM, 50 mM, and 100 mM) of D-glucose (Sigma-Aldrich) dissolved in serum-free DMEM were added to each well and incubated for 24 h. Cell viability was estimated via a colorimetric MTT method. Subsequently, the medium was removed and treated with 50 µL of MTT reagent (2 mg/mL in phosphate-buffered saline [PBS]) for 4 h. Following a removal of MTT, purple crystals were dissolved in 100 µL of DMSO and the absorbance was measured at 540 nm using a micro plate reader (Synergy HT, BioTek Instruments, Winooski, Vermont, USA). Cell viability at different glucose concentrations was expressed as a percentage of the blank (0 mM of glucose).

The cell proliferation was further studied at a glucose concentration of 30 mM. EA.hy926 cells were seeded in six-well plates at a density of 1×10^6 and incubated overnight. The cells were treated with 0 mM and 30 mM of glucose and incubated. After 24 h, the cells were harvested by trypsinization, and then the cells were washed with ice-cold phosphate-buffered saline (PBS) and incubated with Muse™ cell count and viability reagent (Milipore, Manufacturer, Billerica, MA, USA) for five minutes. The cell viability count was measured by Muse™ cell analyzer (Milpore, Hayward, CA, USA).

1.2.7. Analysis of cell viability

The cytotoxicity of IPA in EA.hy926 was assayed by MTT assay. Briefly, 1×10^5 of EA.hy926 cells were seeded in each well of 96-well plates. After the incubation of 24 h, the cells were treated with different concentrations of IPA (0, 0.05, 0.15, 0.5, 1.5, 2.5 μM) with three replicates for each concentration. After 24 h, the medium was replaced with 50 μL of MTT stock solution and incubated for 3 h at 37 °C. The insoluble formazan product was dissolved in 100 μL of DMSO and the absorbance was measured at 540 nm using a microplate reader. The cell viability was expressed as a % of blank (no IPA treatment).

The effect of IPA on high glucose-induced cell proliferation was determined by measuring the cell viability through MTT assay. The cells were treated with 30 mM of glucose to induce the angiogenesis. The cells were treated together with glucose and different concentrations of IPA (0, 0.05, 0.15, 0.5, 1.5 μM). After 24 h of treatment the cell viability was assessed by MTT assay. The cell viability was expressed as a % of the blank (0 mM glucose + 0 μM IPA). The effect of 30 mM glucose for the cell viability was compared with the blank and the effect of IPA on high glucose-induced cells were compared to the control (30 mM glucose + 0 μM IPA).

In further experiments, blank and control treatments are defined as, blank: 0 mM glucose + 0 μM IPA and control: 30 mM glucose + 0 μM IPA.

1.2.8. Scratch-wound cell migration assay

The cell migration was evaluated according to a previously described method with slight modifications [8]. EA.hy926 cells were seeded in 96 well plates and the cells were grown to 80 % confluence. The cell monolayer was scraped at the middle of the well using a sterile 10 μL pipette tip and the cells were washed twice with PBS. The cells were treated

together with glucose and IPA (0.05, 0.15, 0.5, 1.5 μ M). After the sample treatment, the cells were photographed (LIONHEART^{FX} automated live cell imager) and the initial gap length (0 h) was measured (Gen5 3.04). After 12 h incubation, final gap length was measured. The gap width was measured at five different places and averaged. To determine the effect for cell migration, the gap closure % was calculated as follows [21]:

$$\text{Gap Closure \%} = \frac{\text{Initial gap length} - \text{Final gap length}}{\text{Initial gap length}} \times 100\%$$

1.2.9. Tube formation Assay

EA.hy926 cells were seeded on top of Matrigel[®] matrix, in order to determine the effect of IPA in high-glucose induced capillary formation according to a previously described method [22]. Briefly, 96 well plates were coated with 75 μ L of Matrigel per well and polymerized at 37 $^{\circ}$ C for 30 min. The trypsinized EA.hy926 cells were divided into approximately equal number of cells (1×10^5) and the cell pellets were suspended in different treatments of glucose and IPA. After 6 h of incubation, cultures were photographed (4 \times) and analyzed using the plugin “Angiogenesis Analyzer” of image J software. Angiogenic score was calculated as follows [23].

$$\text{Angiogenic Score} = \text{Number of branches} \times \text{Total branch length}$$

1.2.10. In silico docking of VEGFR-2 receptor and IPA

For docking study, the crystal structures of proteins were obtained from Protein Data Bank (PDB, <http://www.pdb.org>) and the blocking of the protein-ligand complex, possibility of binding, precise location of binding site and binding mode of the ligand were examined using Discovery Studio (2018).

1.2.11. Western blot analysis

Protein extraction was done separately for cytosolic proteins and membrane proteins, using a protein extraction kit (MEM-PERTM Plus Kit; Thermo Scientific). The resulted proteins were quantified (PierceTM BCA Protein Assay kit; Thermo Scientific) and equal amount of proteins (30 µg) were separated using 7.5% or 12% SDS-PAGE. The resolved proteins were transferred to nitrocellulose membranes (GE Healthcare Life Science) and blocked for 3 h with nonfat dry milk at RT. Membranes were then incubated for overnight at 4 °C with the following primary antibodies: phosphorylated and /or total VEGFR-2, extracellular signal-regulated kinase (ERK), protein kinase B (AKT), c-Jun N-terminal kinase (JNK), endothelial nitric oxide synthase (eNOS) and Glyceraldehyde 3-phosphate dehydrogenase (GAPDH). Following the incubation with secondary antibodies for 2 h, protein bands were detected with chemiluminescence reagent (Maximum sensitivity substrate, Thermo Scientific) and images were captured using Fusion Solo apparatus (Vilber Lourmat). The relative levels of protein expression were measured using image J software and normalized to respective total form or GAPDH.

1.2.12. Statistical Analysis

The data were analyzed using GraphPad Prism 5 or Microsoft Excel and evaluated using two-way ANOVA and Dunnett's multiple range tests. All the experiments were performed a minimum of three times and expressed as Mean ± standard deviation (SD). ns; not significant, *p < 0.05, **p < 0.01, ***p < 0.001, # p < 0.05, ## p < 0.01, ### p < 0.001.

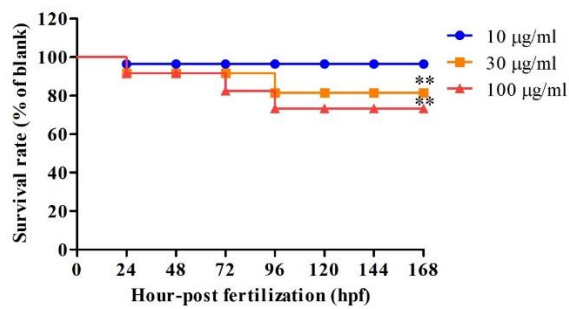
1.3. Results

1.3.1. Effects of IO extract on high glucose-treated zebrafish embryo

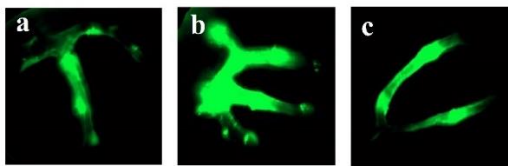
The toxicity of IO extract in transgenic zebrafish (*flk:EGFP*) embryo was investigated using different concentrations of IO extract (10, 30, and 100 $\mu\text{g}/\text{mL}$). As shown in Figure 1-2A, 10 $\mu\text{g}/\text{mL}$ of IO extract showed no significant toxicity in transgenic zebrafish (*flk:EGFP*) embryo, and hence, this concentration was used in further experiments.

Transgenic zebrafish (*flk:EGFP*) embryos were treated with 130 mM glucose [18-19] to induce angiogenesis in the whole body including hyaloid-retinal vessels (Figure 1-2). Treatment with glucose (130 mM) yielded 162.7% of retinal vessel diameter as compared to the blank (no glucose). Treatment with 10 $\mu\text{g}/\text{mL}$ of IO extract significantly suppressed the retinal vessel diameter (99.5% similar to the blank) (Figures 1- 2B, 2C). Fluorescence intensities were measured for the quantitative analysis of vascular growth in the whole body. Treatment with glucose (130 mM) yielded 182.8% fluorescence intensity as compared to the blank (Figures 1D, 1E). Treatment with 10 $\mu\text{g}/\text{mL}$ of IO extract suppressed the high glucose-induced vascular growth in the whole body (107.1% intensity as compared to the blank).

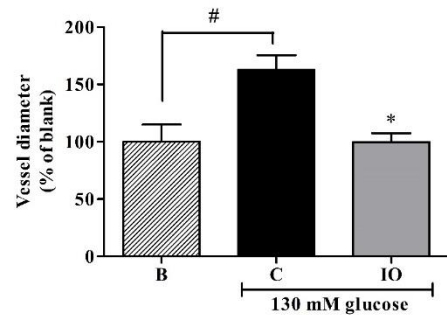
(A)



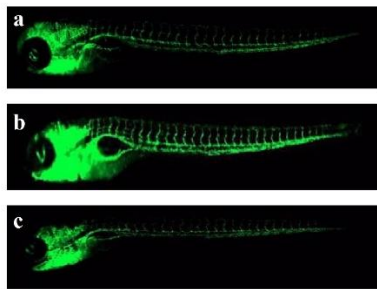
(B)



(C)



(D)



(E)

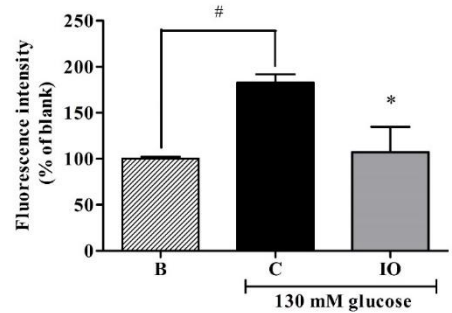


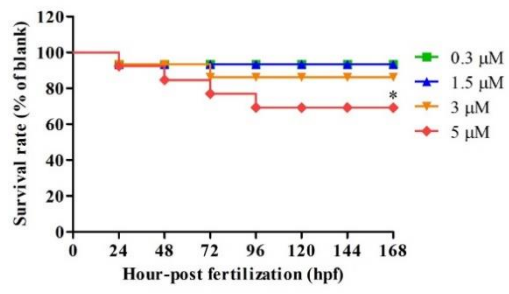
Figure 1-2. Effects of *Ishige okamurae* (IO) extract on zebrafish embryo. (A) Effects of IO extract on the survival rate of transgenic zebrafish (*flk:EGFP*) embryos. The embryos were treated with 10, 30, and 100 µg/mL of IO extract for 24, 48, 72, 96, 120, 144, and 168 hours post fertilization (hpf). The treatment effects were normalized to blank (0 µg/mL IO extract). (B) Fluorescence microscopic images of the retinal vessels of transgenic zebrafish (*flk:EGFP*) embryos treated with IO extract. (C) The diameter of the hyaloid retinal vessel treated with IO extract. (D) Images of the whole body vessel formation in transgenic zebrafish (*flk:EGFP*) embryos treated with IO extract as obtained by fluorescence microscopy. (E) Quantified fluorescence intensity of the whole body treated with IO extract (a: 0 mM glucose + 0 µg/mL IO, b: 130 mM glucose + 0 µg/mL IO, and c: 130 mM glucose + 10 µg/mL IO). The effects of 130 mM glucose on vessel formation were compared with B [blank (0 mM glucose + 0 µg/mL IO extract)]. The effects of IO on high glucose-induced vessel formation were normalized to C [control (130 mM glucose + 0 µg/mL IO extract)].

1.3.2. Effects of IPA on high glucose-treated zebrafish embryo

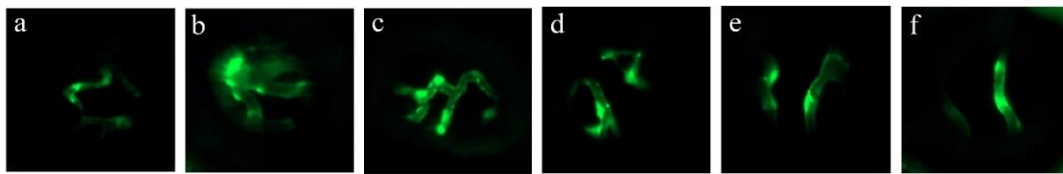
Initially, the toxicity of IPA on transgenic zebrafish (*flk:EGFP*) embryo was investigated with different concentrations of IPA (0.3, 1.5, 3, and 5 μM). The results showed (Figure 1-3A) that up to 3 μM of IPA had no significant toxic effects. Hence, we selected IPA concentrations of 0.015, 0.05, 0.15, and 0.5 μM to evaluate the anti-angiogenic effects in transgenic zebrafish (*flk:EGFP*) embryo.

Glucose treatment yielded 170.4% of retinal vessel diameter. When treated with IPA at concentrations of 0.015, 0.05, 0.15, and 0.5 μM , the retinal vessel diameters were decreased to 144.49, 117.87, 109.14, and 104.36%, respectively as compared to the blank (Figures 1-3B, 3C). The fluorescence intensity of glucose treatment was 157.8%. When treated with IPA at concentrations of 0.015, 0.05, 0.15, and 0.5 μM , the fluorescence intensities were decreased to 155.5, 138.3, 134.4, and 120.9%, respectively. (Figures 1-3D, 3E). After observations of vascular growth in hyaloid-retina and whole body, it could be inferred that treatment with IPA alone leads to anti-angiogenic effects against high glucose-induced angiogenesis.

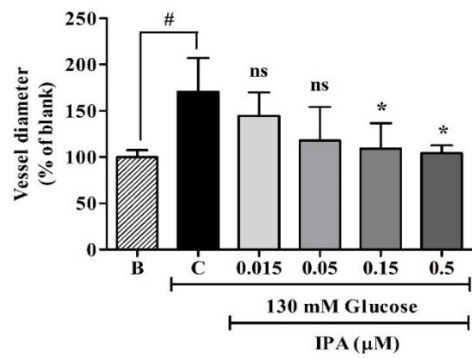
(A)



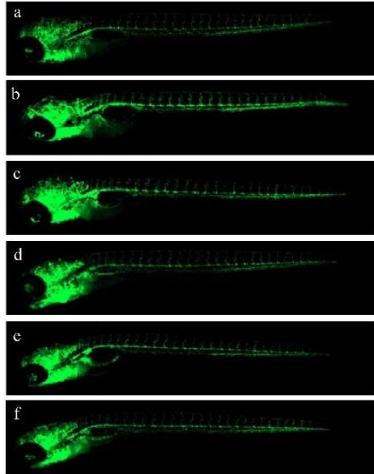
(B)



(C)



(D)



(E)

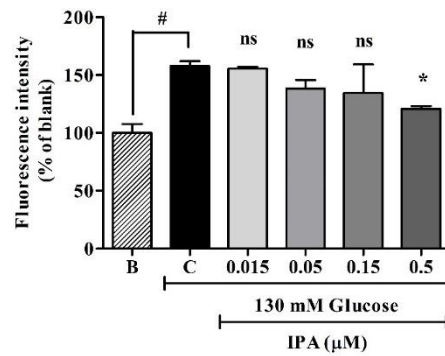
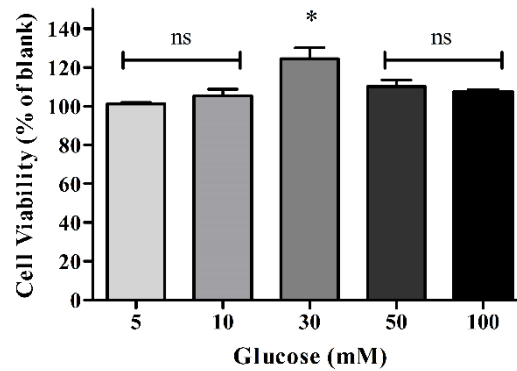


Figure 1- 3. Effects of IPA on transgenic zebrafish (*flk:EGFP*) embryos. (A) Effects of IPA on the survival rate of transgenic zebrafish (*flk:EGFP*) embryos. The embryos were treated with 0.3, 1.5, 3, and 5 μM IPA for 24, 48, 72, 96, 120, 144, and 168 hpf. The treatment effects were normalized to blank (0 μM IPA). (B) Fluorescence microscopic images of the retinal vessels of transgenic zebrafish (*flk:EGFP*) embryos treated with IPA. (C) The diameter of hyaloid retinal vessels treated with IPA. (D) The images of whole body vessel formation in transgenic zebrafish (*flk:EGFP*) embryos treated with IPA as obtained by fluorescence microscopy. (E) Quantified fluorescence intensity of the whole body treated with IO extract (a: 0 mM glucose + 0 μM IPA, b: 130 mM glucose + 0 μM IPA, c: 130 mM glucose + 0.015 μM IPA, d: 130 mM glucose + 0.05 μM IPA, e: 130 mM glucose + 0.15 μM IPA, and f: 130 mM glucose + 0.5 μM IPA). The effects of 130 mM glucose on vessel formation were compared to B [blank (0 mM glucose + 0 μM IPA)]. The effects of IPA on high glucose-induced vessel formation were normalized to C [control (130 mM glucose + 0 μM IPA)].

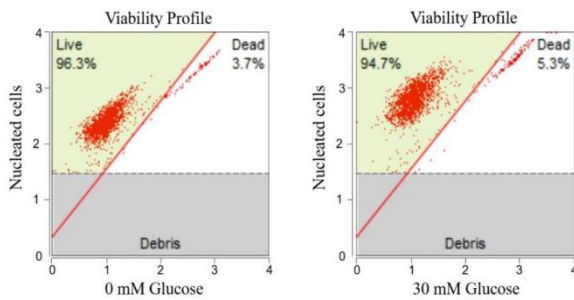
1.3.3. Glucose-Induced Angiogenesis in EA.hy926 Cells

Prior to assessing the anti-angiogenic effects of IO extract and IPA *in vitro*, EA.hy926 cells were treated with different concentrations of glucose (0 mM, 5 mM, 10 mM, 30 mM, 50 mM, and 100 mM) to confirm the concentration that could induce the angiogenesis condition in EA.hy926 cells. According to the MTT (3-[4, 5-dimethylthiazol-2-yl]-2, 5-diphenyltetrazolium bromide) assay results (Figure 1-4A) the endothelial cell viability was significantly increased at 30 mM glucose concentration. After 24 h, EA.hy926 cells showed $124.8 \pm 5.5\%$ of cell viability compared to the blank (no glucose treatment). In order to further confirm the effect of 30 mM of glucose in the cell proliferation, the viable cell count was analyzed using the Muse™ Cell Analyzer, and the results showed a significant cell proliferation at 30 mM of glucose concentration, compared to the blank (Figure 1-4C). These results suggested that 30 mM of glucose could be used for the *in vitro* angiogenesis induction in EA.hy926 cells, and therefore, this concentration was used for further studies.

(A)



(B)



(C)

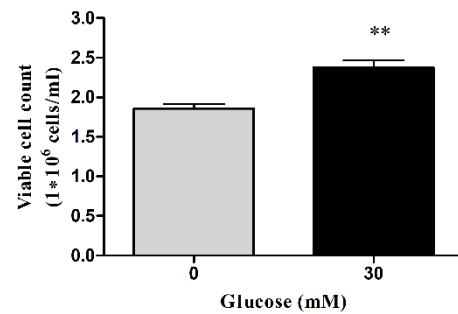


Figure 1-4. Effect of glucose on the proliferation of vascular endothelial cell Ea.hy926. (A) Cell viability upon treatment with glucose for 24 h. Cells were incubated with increasing concentrations of glucose (zero mM, five mM, 10 mM, 30 mM, 50 mM, and 100 mM) for 24 h, and cell viability was determined by the MTT assay. Results are normalized to blank (0 mM of glucose). Cell viability upon the treatment with 30 mM of glucose for 24 h was assessed using the Muse™ Count and Viability Kit; representative viability profiles (dot plots) (B) and viable cell count are shown (C). The results were obtained using Muse™ Cell Analyzer.

1.3.4. Effects of IPA on high glucose-induced cell proliferation, migration, and capillary-like structure formation

MTT assay was performed to evaluate its cytotoxicity in EA.hy926 cells. The cell viability was 92.94%, 91.31%, 90.24%, 86.78%, and 78.48% when treated with IPA at concentrations of 0.05, 0.15, 0.5, 1.5, and 2.5 μM , respectively (Figure 1-4A). The non-toxic IPA concentrations of 0.05, 0.15, 0.5, and 1.5 μM were used in later experiments, as $> 80\%$ cell viability was selected to be used in the cellular experiments [24]. Anti-angiogenesis effect of IPA was evaluated for cell proliferation, cell migration and capillary formation. The cell viability was taken as an indicator of cell proliferation [21]. As shown in Figure 1-4B, significant cell proliferation (124.93%) was observed after treatment with 30 mM glucose. Once the cells were treated together with 30 mM glucose and ascending concentration of IPA, the cell proliferation was decreased significantly in a concentration-dependent manner. The results were 117.12%, 102.95%, 97.80%, and 92.21% when treated with IPA at concentrations of 0.05, 0.15, 0.5, and 1.5 μM , respectively. These results suggest that IPA exerts anti-angiogenic effects by inhibiting high glucose-induced vascular cell proliferation.

Scratch-wound cell migration assay was used to determine the effects of IPA on high glucose-induced cell migration. The cell migration ability was compared by calculating the gap closure percentage (Figures-1 5A, 5B). The higher gap closure percentage indicated higher cell migration ability and vice versa. Higher cell migration was recorded as 22.91% after treatment with 30 mM glucose. It was significantly decreased to 20.42, 17.76, and 16.8%, when treated with IPA at concentrations of 0.05, 0.15, 0.5 and 1.5 μM , respectively.

The vascular endothelial cells cultured in Matrigel[®] matrix can differentiate into capillary-like structures [25]. This characteristic feature was used to evaluate the IPA effects on high glucose-induced capillary-like structure formation (Figures 1- 6A and 6B). The angiogenic score was determined for quantitative evaluation of capillary formation. An increased angiogenic score is an indicator of higher capillary formation. According to the results, a higher angiogenic score was reported as 7.01×10^5 in the cells treated with 30 mM glucose. After IPA treatment, the angiogenic score was significantly decreased. The angiogenic score was 5.47×10^5 , 4.97×10^5 , and 2.47×10^5 when treated with IPA at concentrations of 0.05, 0.15, 0.5, and 1.5 μM , respectively. These data suggest that IPA exerts anti-angiogenic effects by suppressing capillary formation.

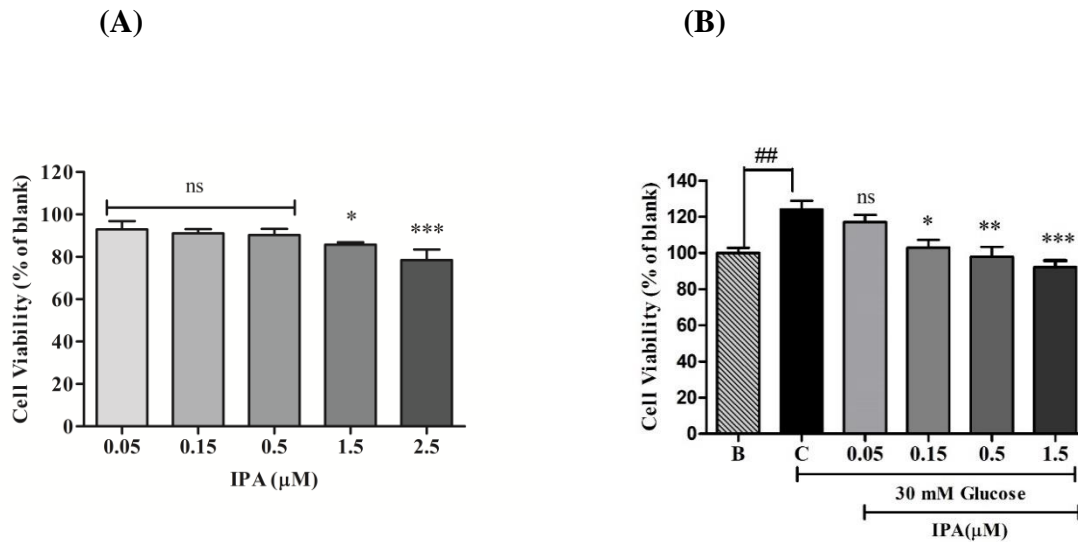
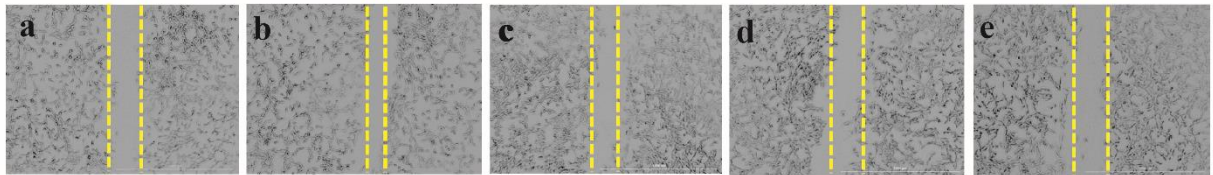


Figure 1-5. IPA inhibits the proliferation of EA.hy926 cells. (A) Cytotoxicity of IPA in EA.hy926 cells. The cells were treated with different IPA concentrations (0, 0.05, 0.15, 0.5, 1.5, and 2.5 μM) for 24 h and the cell viability was determined by MTT assay. The results were normalized to blank (0 μM IPA). (B) IPA inhibits the proliferation of high glucose-induced EA.hy926 cells. The cells were treated with different concentrations of IPA (0.05, 0.15, 0.5, and 1.5 μM) along with 30 mM glucose. MTT assay was performed to determine cell viability. The anti-proliferative effects of IPA in high glucose-induced cells were normalized to C [control (30 mM glucose + 0 μM IPA)] and the effects of 30 mM glucose were compared to B [blank (0 mM glucose + 0 μM IPA)].

(A)



(B)

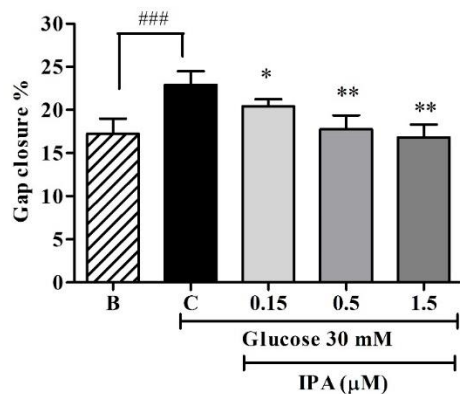
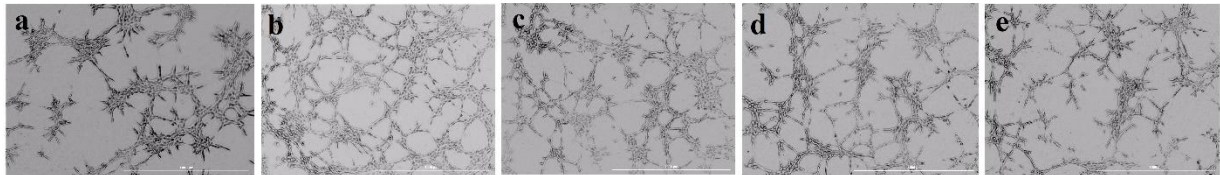


Figure 1-6. (A) IPA inhibits high glucose-induced cell migration. The cells were treated with different concentrations of IPA (0.15, 0.5, and 1.5 μM) along with 30 mM glucose. The cell monolayer was scraped at the middle of the well and the initial gap length (0 h) and the final gap length (12 h) was measured. (B) The gap closure was quantified by percentage (%). The effects of 30 mM glucose on cell migration were compared to B [blank (0 mM glucose + 0 μM IPA)], The effects of IPA on high glucose-induced cell migration were normalized to C [control (30 mM glucose + 0 μM IPA)].

(A)



(B)

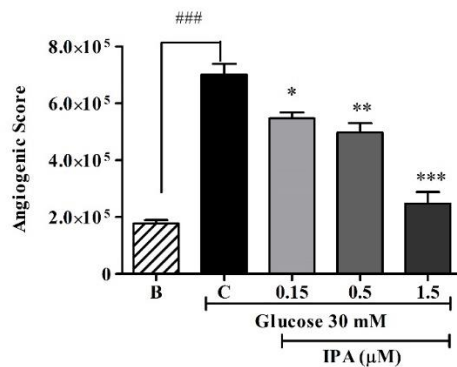
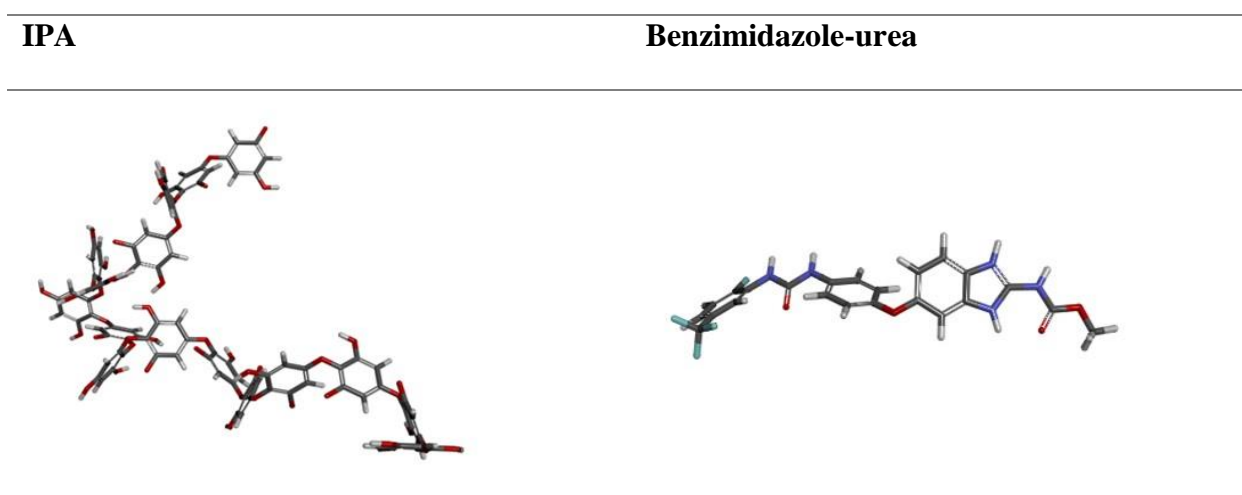


Figure 1-7. (A) IPA suppresses high glucose-induced capillary formation in Matrigel®. The cells were seeded on Matrigel® with different concentrations of IPA (0.15, 0.5, and 1.5 μM) along with 30 mM glucose including B [blank (0 mM glucose + 0 μM IPA)] and C [control (30 mM glucose + 0 μM IPA)]. After 6 h incubation, the cells were photographed and the angiogenic score was determined. (B) Quantification of capillary formation. The effects of 30 mM glucose on capillary formation were compared to B [blank (0 mM glucose + 0 μM IPA)]. The effects of IPA on high glucose-induced capillary formation were normalized to C [control (30 mM glucose + 0 μM IPA)].

1.3.5. Analysis of molecular docking of IPA and VEGFR-2 Receptor

In order to gain more insights of the binding modes of VEGFR2 and IPA, an in silico study of molecular docking was performed. For the docking comparison, benzimidazole-urea was used [26]. The crystal structure of VEGFR-2 was obtained from Protein Data Bank (PDB: ID 2OH4). Simulations of the docking of various VEGFR-2 and IPA complexes were performed by fitting IPA into the active site of VEGFR-2. The structures of IPA and benzimidazole-urea are shown in Table 1.

Based on the best docking mode of the complex two types of energy values were expressed (Table 2). CDOCKER energy values were -656.93 kcal/mol, -57.09 kcal/mol respectively for IPA and benzimidazole-urea while binding energy values were -143.419 kcal/mol, -57.09 kcal/mol respectively for IPA and benzimidazole-urea.

Table 1. Ligands; IPA, Benzimidazole-urea**Table2.** The calculated affinities for VEGFR-2

No.	Ligands	Pose	Binding energy (kcal/mol)	CDOCKER interaction energy (kcal/mol)
1	IPA	16	-656.948	-656.935
2	Benzimidazole-urea	106	-143.419	-57.0972

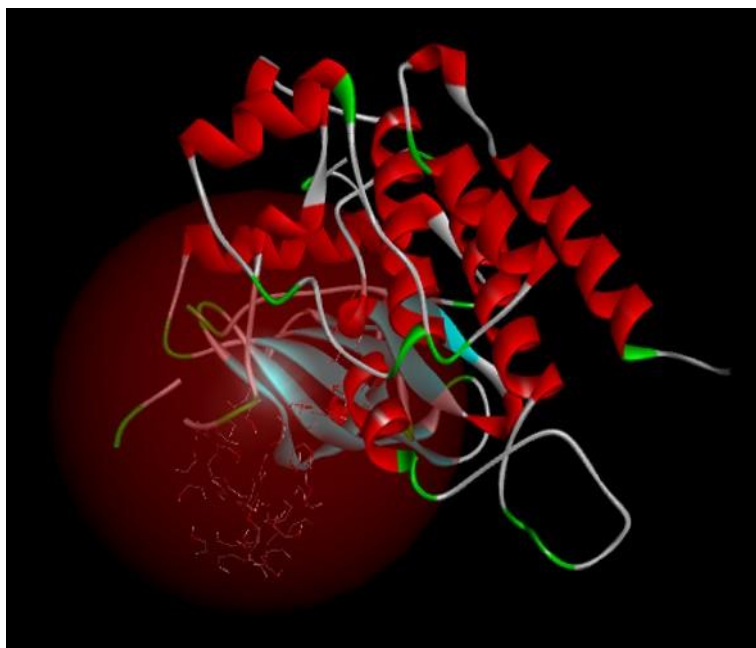
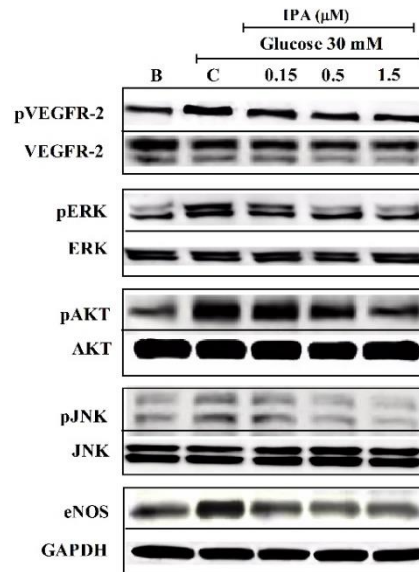


Figure 1-8. Computational prediction of the VEGFR-2 receptor and docking simulation with IPA

1.3.6. Effects of IPA on VEGFR-2 and downstream signaling cascade

The expression of pVEGFR2 and its downstream signaling molecules were detected using western blotting (Figure 1-7). pVEGFR-2 expression was significantly increased in the high glucose-treated EA.hy926 cells as compared to the blank. As shown in Figure 6B, high glucose-induced pVEGFR-2 expression was decreased significantly in the cells treated with IPA. In addition, high glucose treatment showed higher protein expression in the downstream signaling molecules AKT, ERK, JNK, and eNOS. With IPA treatment these parameters were significantly down-regulated.

(A)



(B)

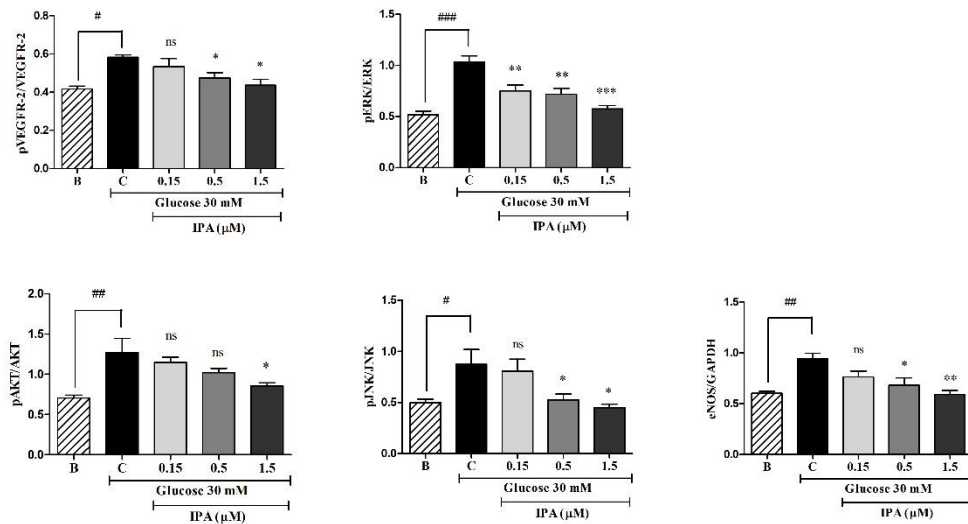


Figure 1-9. (A) IPA inhibits VEGFR-2 and its downstream signaling molecules. IPA attenuating high glucose-induced phosphorylation of VEGFR-2 and downstream signaling molecules ERK, AKT, JNK, and eNOS were detected using western blotting. (B) Quantitative evaluation of the protein expression. The effects of 30 mM glucose on the expression of each protein were compared to B [blank (0 mM glucose + 0 μM IPA)]. The effects of IPA on high glucose-induced protein expression were normalized to C [control (30 mM glucose + 0 μM IPA)].

1.4. Discussion

Previous studies have demonstrated that seaweeds are rich in bioactive components having medicinal values [27]. IO has long been used as an edible seaweed in Korea. According to previous studies, ethanolic extract of IO possess a therapeutic potential in treating chronic inflammation [28]. A recent study has shown that the ethanolic extract of IO possesses anti-diabetic activities by inhibiting α -glucosidase [14]. Till date, to our knowledge, there is no study demonstrating the anti-angiogenic effects of the ethanolic extract of IO. Here for the first time, we demonstrated the anti-angiogenic effects of the ethanolic extract of IO on high glucose-induced-angiogenesis.

IPA is a phlorotannin isolated from the IO extract, it is known for its α -glucosidase inhibitory activity and constitutes 1.8 % of IO [14]. Treatment with 10 μ g/mL of IO extract showed anti-angiogenic effects against high glucose-induced vascular growth. Upon this observation, we hypothesized that IPA from IO extract could be the key molecule attributed to the anti-angiogenic effects.

IPA contains hydroxyl groups bonded with its benzene structure (Supplementary Figure 1). The comparatively higher number of hydroxyl groups may be advantageous to its biological activities. It has been reported that phlorotannins, which contain >10 hydroxyl groups, show higher anti-oxidant activities [29]. Analysis of our data revealed that IPA exerted anti-angiogenic effects in the concentration range of 0.05–0.15 μ M. This approximately represents 0.1–0.3 μ g/mL of IPA (molecular weight of IPA, 1984 g/mL). Therefore, the anti-angiogenic effects of IO extract could be attributed to the IPA present in the IO extract. Further studies were carried out with IPA in vascular endothelial cells EA.hy926 to evaluate the cellular mechanisms against high glucose-induced angiogenesis.

Angiogenesis is a step by step process of cell proliferation, migration, and capillary formation [30]. In angiogenesis, cell migration is an essential event where the cells are moved towards a controlled direction before capillary morphogenesis [31]. IPA significantly reduced the high glucose-induced cell migration. Furthermore, capillary formation was evaluated as in the process of developing drugs targeting angiogenesis, the 3D capillary formation is an important aspect [32]. Overall our data showed that IPA was efficacious in inhibiting high glucose-induced endothelial cell proliferation, migration, and capillary formation.

The molecular docking study was performed to evaluate the binding of IPA to VEGFR-2. It results lower binding energy and CDOCKER interaction energy compared to Benzimidazole-urea (comparison molecule). This means that the binding of IPA and VEGFR-2 is more stable and results anti-angiogenesis effects.

According to previous supporting evidence [33] downstream signaling mediators of VEGFR-2 including ERK, AKT, JNK, and eNOS are involved in the regulation of endothelial cell proliferation and survival. ERK and JNK are actively involved in endothelial cell proliferation [34], whereas AKT shows an important role in endothelial cell survival [35]. eNOS is involved in the production of large amounts of NO in the endothelial cells and plays a critical role in all the processes of angiogenesis including the breakup of the matrix, endothelial cell migration, proliferation, network structure organization, and lumen formation [36].

In mammals, three different VEGF-receptors are found, namely, VEGFR-1, VEGFR-2, and VEGFR-3. VEGFR-1 is important for hematopoietic cell development and VEGFR-3 is crucial for lymphatic endothelial cell development. The VEGFR-2 is the principal receptor involved in endothelial cell development and attracts much attention in the anti-angiogenic

therapeutic intervention [37]. Bevacizumab is an example of a drug that targets VEGFR inhibition although it causes several adverse effects, such as hypertension, fatigue, rash, and myalgia due to lack of target specificity [38]. Therefore, nowadays, interventions by anti-angiogenic drugs obtained from natural compounds are much preferred because of the low adverse effects profile. Qi, et al. [8] has reported the anti-angiogenic effects of a marine bromophenol bis (2,3-dibromo-4,5-dihydroxybenzyl) ether in vascular endothelial cells through suppressing VEGFR signaling pathway. Our results demonstrated that IPA, isolated from a marine alga, exerts its anti-angiogenic effects by interfering with the VEGFR-2 signaling pathway.

Conclusion

The findings of the present study demonstrated the anti-angiogenic effects of a marine source. *Ishige okamurae* (IO) extract attenuated high glucose-induced vascular growth in transgenic zebrafish (*flk:EGFP*). IPA isolated from IO extract exerted anti-angiogenic effects against high glucose-induced angiogenesis. Further, the anti-angiogenic mechanism of IPA in the vascular endothelial cells showed that IPA suppressed high glucose-induced cell proliferation, cell migration, and capillary formation which are known to be the key steps involved in angiogenesis. Additionally, in silico analysis showed IPA inhibits the vascular endothelial receptor, VEGFR-2. IPA treatment suppressed VEGFR-2 receptor expression and downstream signaling cascade in high glucose-induced vascular endothelial cells. Thus, IO extract and IPA could be developed as potential therapeutic candidates for diabetes-related angiogenesis.

References

- 1 ELLIS L: Overview of angiogenesis: Biologic implications for antiangiogenic therapy. *Semin Oncol* 2001;28:94–104.
- 2 Tomanek RJ, Schatteman GC: Angiogenesis: New insights and therapeutic potential. *Anat Rec* 2000;261:126–135.
- 3 Kota SK, Meher LK, Jammula S, Kota SK, Krishna SVS, Modi KD: Aberrant angiogenesis: The gateway to diabetic complications. *Indian J Endocrinol Metab* 2012;16:918–30.
- 4 Costa PZ, Soares R: Neovascularization in diabetes and its complications. Unraveling the angiogenic paradox. *Life Sci* 2013;92:1037–1045.
- 5 Lee R, Wong TY, Sabanayagam C: Epidemiology of diabetic retinopathy, diabetic macular edema and related vision loss. *Eye Vis* 2015;2:17.
- 6 Zent R, Pozzi A: Angiogenesis in Diabetic Nephropathy. *Semin Nephrol* 2007;27:161–171.
- 7 Loges S, Schmidt T, Carmeliet P: Mechanisms of Resistance to Anti-Angiogenic Therapy and Development of Third-Generation Anti-Angiogenic Drug Candidates. *Genes Cancer* 2010;1:12–25.
- 8 Qi X, Liu G, Qiu L, Lin X, Liu M: Marine bromophenol bis(2,3-dibromo-4,5-dihydroxybenzyl) ether, represses angiogenesis in HUVEC cells and in zebrafish embryos via inhibiting the VEGF signal systems. *Biomed Pharmacother* 2015;75:58–66.
- 9 Sugawara T, Matsubara K, Akagi R, Mori M, Hirata T: Antiangiogenic Activity of Brown Algae Fucoxanthin and Its Deacetylated Product, Fucoxanthinol. *J Agric Food Chem* 2006;54:9805–9810.

- 10 Madonna R, Giovannelli G, Confalone P, Renna FV, Geng Y-J, De Caterina R: High glucose-induced hyperosmolarity contributes to COX-2 expression and angiogenesis: implications for diabetic retinopathy. *Cardiovasc Diabetol* 2016;15:18.
- 11 Heo S-J, Kim J-P, Jung W-K, Lee N-H, Kang H-S, Jun E-M, et al.: Identification of chemical structure and free radical scavenging activity of diphlorethohydroxycarmalol isolated from a brown alga, *Ishige okamurae*. *J Microbiol Biotechnol* 2008 [cited 2019 Feb 6];18:676–81.
- 12 Kim M-M, Rajapakse N, Kim S-K: Anti-inflammatory effect of *Ishige okamurae* ethanolic extract via inhibition of NF- κ B transcription factor in RAW 264.7 cells. *Phyther Res* 2009;23:628–634.
- 13 Park MH, Jeon Y-J, Kim H-J, Han JS: Effect of Diphlorethohydroxycarmalol Isolated From *Ishige okamurae* on Apoptosis in 3 t3-L1 Preadipocytes. *Phyther Res* 2013;27:931–936.
- 14 Ryu B, Jiang Y, Kim H-S, Hyun J-M, Lim S-B, Li Y, et al.: Ishophloroglucin A, a Novel Phlorotannin for Standardizing the Anti- α -Glucosidase Activity of *Ishige okamurae*. *Mar Drugs* 2018;16:436.
- 15 Edgell C-JS, Mcdonald CC, Graham JB: Permanent cell line expressing human factor VIII-related antigen established by hybridization (endothelium/somatic cell genetics/differentiated cell lines/von Willebrand factor/hemostasis). *Cell Biol* 1983 [cited 2018 May 27];80:3734–3737.
- 16 Edgell CJS, Haizlip JE, Bagnell CR, Pakenham JP, Harrison P, Wilbourn B, et al.: Endothelium specific Weibel-Palade bodies in a continuous human cell line, EA.hy926. *Vitr Cell Dev Biol* 1990;26:1167–1172.

- 17 ARANDA E, OWEN GI: A semi-quantitative assay to screen for angiogenic compounds and compounds with angiogenic potential using the EA.hy926 endothelial cell line. *Biol Res* 2009;42:377–389.
- 18 Eremeeva ME, Silverman DJ: Rickettsia rickettsii infection of the EA.hy 926 endothelial cell line: morphological response to infection and evidence for oxidative injury. [cited 2018 Sep 13]. Available from: www.microbiologyresearch.org
- 19 Paz K, Zhu Z: Development Of Angiogenesis Inhibitors To Vascular Endothelial Growth Factor Receptor 2. Current Status And Future Perspective. *Front Biosci* 2005;10:1415–1439.
- 20 Jung S-H, Kim YS, Lee Y-R, Kim JS: High glucose-induced changes in hyaloid-retinal vessels during early ocular development of zebrafish: a short-term animal model of diabetic retinopathy. *Br J Pharmacol* 2016;173:15–26.
- 21 Fernando K, Yang H-W, Jiang Y, Jeon Y-J, Ryu B, Fernando KHN, et al.: Diphlorethohydroxycarmalol Isolated from *Ishige okamurae* Represses High Glucose-Induced Angiogenesis In Vitro and In Vivo. *Mar Drugs* 2018;16:375.
- 22 Okamoto T, Akita N, Kawamoto E, Hayashi T, Suzuki K, Shimaoka M: Endothelial connexin32 enhances angiogenesis by positively regulating tube formation and cell migration 2014; DOI: 10.1016/j.yexcr.2013.12.002
- 23 Erices R, Cubillos S, Aravena R, Santoro F, Marquez M, Orellana R, et al.: Diabetic concentrations of metformin inhibit platelet-mediated ovarian cancer cell progression. *Oncotarget* 2017;8:20865–20880.
- 24 Oh S-H, Ryu B, Ngo D-H, Kim W-S, Kim DG, Kim S-K: 4-hydroxybenzaldehyde-chitoooligomers suppresses H₂O₂-induced oxidative damage in microglia BV-2 cells.

- Carbohydr Res 2017;440–441:32–37.
- 25 Arnaoutova I, George J, Kleinman HK, Benton G: The endothelial cell tube formation assay on basement membrane turns 20: state of the science and the art. *Angiogenesis* 2009;12:267–274.
- 26 Choi H-E, Choi J-H, Lee JY, Kim JH, Kim JH, Lee JK, et al.: Synthesis and evaluation of nicotinamide derivative as anti-angiogenic agents. *Bioorg Med Chem Lett* 2013;23:2083–2088.
- 27 Mohamed S, Hashim SN, Rahman HA: Seaweeds: A sustainable functional food for complementary and alternative therapy. *Trends Food Sci Technol* 2012;23:83–96.
- 28 Kim M-M, Rajapakse N, Kim S-K: Anti-inflammatory effect of *Ishige okamurae* ethanolic extract via inhibition of NF- κ B transcription factor in RAW 264.7 cells. *Phyther Res* 2009;23:628–634.
- 29 Li Y, Qian Z-J, Ryu B, Lee S-H, Kim M-M, Kim S-K: Chemical components and its antioxidant properties in vitro: An edible marine brown alga, *Ecklonia cava*. *Bioorg Med Chem* 2009;17:1963–1973.
- 30 Liu J-J, Huang T-S, Cheng W-F, Lu F-J: Baicalein and baicalin are potent inhibitors of angiogenesis: Inhibition of endothelial cell proliferation, migration and differentiation. *Int J Cancer* 2003;106:559–565.
- 31 Shibuya M, Claesson-Welsh L: Signal transduction by VEGF receptors in regulation of angiogenesis and lymphangiogenesis. *Exp Cell Res* 2006;312:549–560.
- 32 Del Amo C, Borau C, Gutiérrez R, Asín J, García-Aznar JM: Quantification of angiogenic sprouting under different growth factors in a microfluidic platform. *J Biomech* 2016;49:1340–1346.

- 33 Wang N, Mo ZWS, Yung T, Luo DWH, Chen DYY: Ellagic acid , a phenolic compound , exerts anti-angiogenesis effects via VEGFR-2 signaling pathway in breast cancer 2012;943–955.
- 34 ZHANG W, LIU HT: MAPK signal pathways in the regulation of cell proliferation in mammalian cells. *Cell Res* 2002;12:9–18.
- 35 Gerber HP, McMurtrey A, Kowalski J, Yan M, Keyt BA, Dixit V, et al.: Vascular endothelial growth factor regulates endothelial cell survival through the phosphatidylinositol 3'-kinase/Akt signal transduction pathway. Requirement for Flk-1/KDR activation. *J Biol Chem* 1998;273:30336–43.
- 36 Papapetropoulos A, García-Cardena G, Madri JA, Sessa WC: Nitric oxide production contributes to the angiogenic properties of vascular endothelial growth factor in human endothelial cells. *J Clin Invest* 1997;100:3131–9.
- 37 Holmes K, Roberts L, Thomas AM, Cross MJ: Vascular endothelial growth factor receptor-2: Structure, function, intracellular signalling and therapeutic inhibition 2007; DOI: 10.1016/j.cellsig.2007.05.013
- 38 Cabebe E, Wakelee H: Role of Anti-angiogenesis Agents in Treating NSCLC: Focus on Bevacizumab and VEGFR Tyrosine Kinase Inhibitors. *Curr Treat Options Oncol* 2007;8:15–27.

Chapter-2

Attenuation of diabetic retinopathy by *Ishige okamurae* extract and its

Constituent Ishophloroglucin A

Abstract

Background:

Diabetic retinopathy can cause severe damage to the eyes causing eventual vision loss. *Ishige okamurae* (IO) extract and Ishophloroglucin A (IPA) isolated from IO have been studied for the effects of high glucose-induced angiogenesis and they have exhibited anti-angiogenesis effects. In the present study, IO extract and IPA were studied for the therapeutic effect against diabetic retinopathy.

Methods: Human Retinal Microvascular Endothelial (HRME) cells were treated with 30 mM glucose to mimic diabetic retinopathy. Anti-angiogenesis effects of IO extract IPA were evaluated for cell proliferation, migration and capillary formation. IPA was further studied for the inhibition of NO and suppression of vascular permeability in vitro. The inhibition of vascular permeability by IPA was studied in vivo in transgenic zebrafish (*flk:EGFP*) embryo treated with CoCl₂ and tetramethylrhodamine (TAMRA) dextran.

Results: IO extract and IPA exhibited anti-angiogenesis effects by suppressing cell proliferation, cell migration and capillary formation in high glucose-treated HRMECs. Further IPA inhibited NO production in high glucose-treated HRMECs. IPA down regulated vascular permeability in hypoxia induced transgenic zebrafish (*flk:EGFP*) embryo.

Conclusion: IO extract and IPA can be used to develop therapeutic against diabetic retinopathy

Keywords: *Ishige okamurae*, Ishophloroglucin A, Diabetic retinopathy, Angiogenesis

2.1. Introduction

Diabetes mellitus is a complex metabolic disease affects 170 million people around the world causing several pathological diseases including nephropathy, retinopathy, and cardiovascular diseases [1]. The most frequent cause of blindness among adults is diabetic retinopathy. All the patients with type 1 diabetes and >60% of patients with type 2 diabetes have retinopathy during the first two decades of disease [2]. The progression of diabetic retinopathy is related to abnormalities of the vasculature including permeability of the blood retina barrier (BRB), progressive microvascular damage with vascular endothelial cell and pericyte loss, subsequent occlusion of capillaries, thickening of vascular basement membrane (BM) and excessive retinal neuronal and glial abnormalities [3].

From the previous chapter we could conclude IO extract attenuated high glucose-induced vascular growth in transgenic zebrafish (*flk:EGFP*) and IPA isolated from IO extract exerted anti-angiogenic effects. In this chapter, anti-angiogenesis effects of IO and IPA was evaluated in the condition of diabetic retinopathy. Therefore, Human Retinal Microvascular cells (HRMEC) were treated with high glucose condition to mimic the diabetic retinopathy in vitro.

The appearance of nonspecific microaneurysms is the first clinical sign of diabetic retinopathy. Continues change in the microaneurysms promotes the rupture in the capillaries and forms of intraretinal hemorrhages. When the disease is progressing, the tight junction between the endothelial and the capillaries breaks and accumulates intraretinal fluid. This is a sign of progression of diabetic retinopathy, including the formation of hard exudates. As the disease progresses to proliferative diabetic retinopathy, occlusion of the capillaries leads to hypoxia. Therefore the release of vascular endothelial growth factor (VEGF) resulting in the formation of new retinal blood vessels (neovascularization), these are leaky blood vessels causing hemorrhage that is complicating the disease more [4].

During diabetic retinopathy, NO production leads to vascular protein leakage and increased microvascular permeability [5]. NOS inhibitors are considered as the treatments for diabetic retinopathy [6]. Therefore we evaluated the NO inhibition of IPA in the high glucose treated HRMECs. The inhibition of vascular permeability by IPA was determined in vivo by treating transgenic zebrafish (*flk:EGFP*) embryo with CoCl_2 and tetramethylrhodamine (TAMRA) dextran.

2.2. Materials and Methods

2.2.1. Cell culture

HRMECs (Cat. No. ACBRI 181) were purchased from Cell Systems (Kirkland, WA) and used at passages 3–7. Cells were grown in Complete Classic Medium of Cell Systems (4Z0-500) containing Bac-Off® antibiotic (4Z0-643). Cultures were maintained at 37°C in a humidified 95% air and 5% CO₂ atmosphere.

2.2.2. Cell treatment with glucose

HRME cells were plated onto a 96-well plate with three replicates for each concentration. Following 24 h of incubation at 37 °C, different concentrations (0 mM, 25 mM, 30 mM, 50 mM, and 100 mM) of D-glucose (Sigma-Aldrich) dissolved in serum-free Complete Classic Medium were added to each well and incubated for 24 h. Cell viability was estimated via a colorimetric MTT method [7]. Subsequently, the medium was removed and treated with 50 µL of MTT reagent (2 mg/mL in phosphate-buffered saline [PBS]) for 4 h. Following a removal of MTT, purple crystals were dissolved in 100 µL of DMSO (Amresco, life sciences, Solon, Ohio, USA), and the absorbance was measured at 540 nm using a micro plate reader (Synergy HT, BioTek Instruments, Winooski, Vermont, USA). Cell viability at different glucose concentrations was expressed as a percentage of the blank (0 mM of glucose).

2.2.3. Determination of cytotoxicity of IO extract and IPA in HRMECs

HRME cells (1×10^5 cells/well) were seeded in a 96-well plate and incubated for 24 h. The cells were treated with various concentrations of IO extract (3 µg/ml, 10 µg/ml, 30 µg/ml, 50 µg/ml, 100 µg/ml, 150 µg/ml) and IPA (0 µM, 0.15 µM, 0.5 µM, 1.5 µM, 5 µM, and 15

μM) and further incubated for 24 h. Subsequently, cell viability was determined using the MTT assay as described above (2.2.2), and was expressed as a percentage of the blank (No sample treatment).

2.2.4. Determination of anti-proliferative activity

To assess whether IO extract and IPA affects high glucose-induced cell proliferation, HRME cells were treated with glucose (30 mM) and IO extract (50 μg/ml, 100 μg/ml, 150 μg/ml) or IPA (0.15 μM, 0.5 μM, 1.5 μM) with the blank (neither glucose nor sample) and control (30 mM glucose + 0 sample). Cells were incubated for 24 h and cell viability was measured by the MTT assay as described above (Section 2.3), and expressed as a percentage of the blank. The effect of 30 mM of glucose was compared with the blank. The anti-proliferative effect of DPHC on high glucose-induced proliferation was compared to the control.

2.2.5. Scratch wound cell migration assay

HRME cells were seeded in a 96-well plate at a density of 1×10^5 per well. After obtaining 80% cell confluence, a scratch was made in the middle of the well by a 10 μL tip. After scrapping, cells were washed with PBS twice, and incubated with serum free complete classic medium containing glucose (30 mM) together with IO extract (50 μg/ml, 100 μg/ml, 150 μg/ml) or IPA (0.15 μM, 0.5 μM, 1.5 μM) with the blank (neither glucose nor sample) and control (30 mM glucose + 0 sample). The initial gap width (at 0 h) and the final gap width (after 12 h) were assessed using photography, and gap lengths were quantified using the image J software at three different points and averaged. The gap closure percentage was calculated as follows:

$$\text{Gap Closure \%} = \frac{\text{Initial gap length} - \text{Final gap length}}{\text{Initial gap length}} \times 100\%$$

2.2.6. Tube formation Assay

The tube formation assay was performed using the capillary-like structure formation ability of HRME cells in Matrigel. A 96-well plate was coated with Matrigel (BD Biosciences) and allowed to polymerize by incubating at 37 °C for 30 min. Confluent HRME cells, cultured in T75 flasks, were trypsinized and diluted in Serum free complete classic medium. The cell suspension was divided into 15-mL Falcon tubes containing an equal number of cells (3×10^3) and centrifuged. Cell pellets were suspended in different solutions including the blank, control and different concentrations of IO extract (50 µg/ml, 100 µg/ml, 150 µg/ml) or IPA (0.15 µM, 0.5 µM, 1.5 µM) together with 30 mM of glucose. Cells were then seeded on Matrigel-coated wells and incubated for six hours. Cultures were photographed using 4× magnification, and all of the results were quantified using the plug-in “Angiogenesis Analyzer” from the image J. Angiogenic score was determined by using the following formula [8]:

$$\text{Angiogenic Score} = \text{Number of branches} \times \text{Total branch length}$$

2.2.7. NO inhibition by IPA

In order to determine NO inhibition in high glucose-induced HRME cells by IPA, NO production was measured using two different methods. HRME cells were seeded in 24-well plates with the density of 5×10^4 cells/well. After 24 h incubation, cells were treated with IPA (0.15 µM, 0.5 µM, 1.5 µM) together with 30 mM of glucose including blank and control. The nitrite accumulation in the supernatant was assessed by Griess reagent [0.1%

N-(1-naphthyl)-ethylenediamine, 1% sulfanilamide in 5 % phosphoric acid]. For more efficient detection of NO, fluorescent probe, 4-amino-5-methyamino-2',7'-difluorofluorescein diacetate (DAF-FM DA) [9] was used. After the sample treatment cells were incubated with 1.5 μ M of DAF-FM DA. The excess probe on the cells were washed with PBS and incubated for another 15 mins and fluorescence was measured using a fluorescence plate reader with an excitation wave length of 485nm and an emission wavelength of 520 nm.

2.2.8. Western blotting

After 24 h of incubation, cells were harvested and protein was extracted. The resulting protein content was quantified by a PierceTM BCA protein Assay Kit (Thermo Scientific). An equal amount of cytosolic proteins and membrane proteins (30 μ g) were separated using 12% SDS-PAGE and transferred to the nitrocellulose blotting membrane (GE Healthcare Life Science). Membranes were blocked with non-fat dry milk for 3 h at room temperature and incubated with primary antibodies, including eNOS, and GAPDH (Cell signaling Technology). After overnight incubation at 4 °C, membranes were then incubated with respective secondary antibodies conjugated to horseradish peroxidase for 2 h at room temperature and developed with chemiluminescence reagent (maximum sensitivity substrate, Thermo Scientific, Rockford, IL, USA). Immunoreactive bands were then visualized by a Fusion Solo apparatus (Vilber Lourmat, Collegien, France). The protein expression was normalized to GAPDH using the image J software (NIH, Bethesda, MD, USA).

2.2.9. *In vivo inhibition of vascular permeability by IPA*

Transgenic zebrafish (*flk:EGFP*) embryos were treated with CoCl_2 and tetramethylrhodamine (TAMRA) dextran. Zebrafish transgenic (*flk:EGFP*) embryos [1 day post fertilization (dpf)] were maintained in embryonic water containing 0.3 mM CoCl_2 with different concentrations of IPA (0.015, 0.05, 0.15, 0.5 μM). After 2 days of the treatment embryos were treated with 0.075 mg/ml of Dextran and after 15 min, the images were taken using the fluorescence microscope using two different filters (GFP.469, 525 and RFP.531, 593). Finally the merged images were generated. The fluorescence intensities of the images were measured using Image J software.

2.2.10. *Statistical Analysis*

Data analysis was performed using GraphPad Prism or Microsoft Excel. Data were expressed as mean \pm SD from three independent experiments and analyzed statistically using two-way ANOVA, and significant differences between treatment means were determined using Dunnett's multiple range tests. Significance was accepted at $P < 0.05$ levels.

2.3. Results

2.3.1. Glucose-Induced Angiogenesis in HRME Cells and Cytotoxicity of IO extract and IPA in HRME cells

Prior to assessing the antiangiogenic effects of iO extract and IPA in vitro, HRME cells were treated with different concentrations of glucose (25 mM, 30 mM, 50 mM, and 100 mM) to confirm the concentration that could induce the angiogenesis condition in the retinal endothelial cells. According to the MTT assay results (Figure 2-1A) the endothelial cell viability was significantly increased at 30 mM glucose concentration. After 24 h, HRME cells showed 125.05 % of cell viability compared to the blank (no glucose treatment). The MTT method was used to determine the cytotoxicity of IO extract and IPA in HRME cells. Cells were treated with and IO extract (3 µg/ml, 10 µg/ml, 30 µg/ml, 50 µg/ml, 100 µg/ml, 150 µg/ml), IPA (0 µM, 0.15 µM, 0.5 µM, 1.5 µM, 5 µM, and 15 µM) for 24 h and normalized to the blank. Based on these results, IO, 30 µg/ml, 50 µg/ml, 100 µg/ml, 150 µg/ml and IPA, 0.15 µM, 0.5 µM, 1.5 µM concentrations were selected to assess the anti-angiogenic effect in vitro.

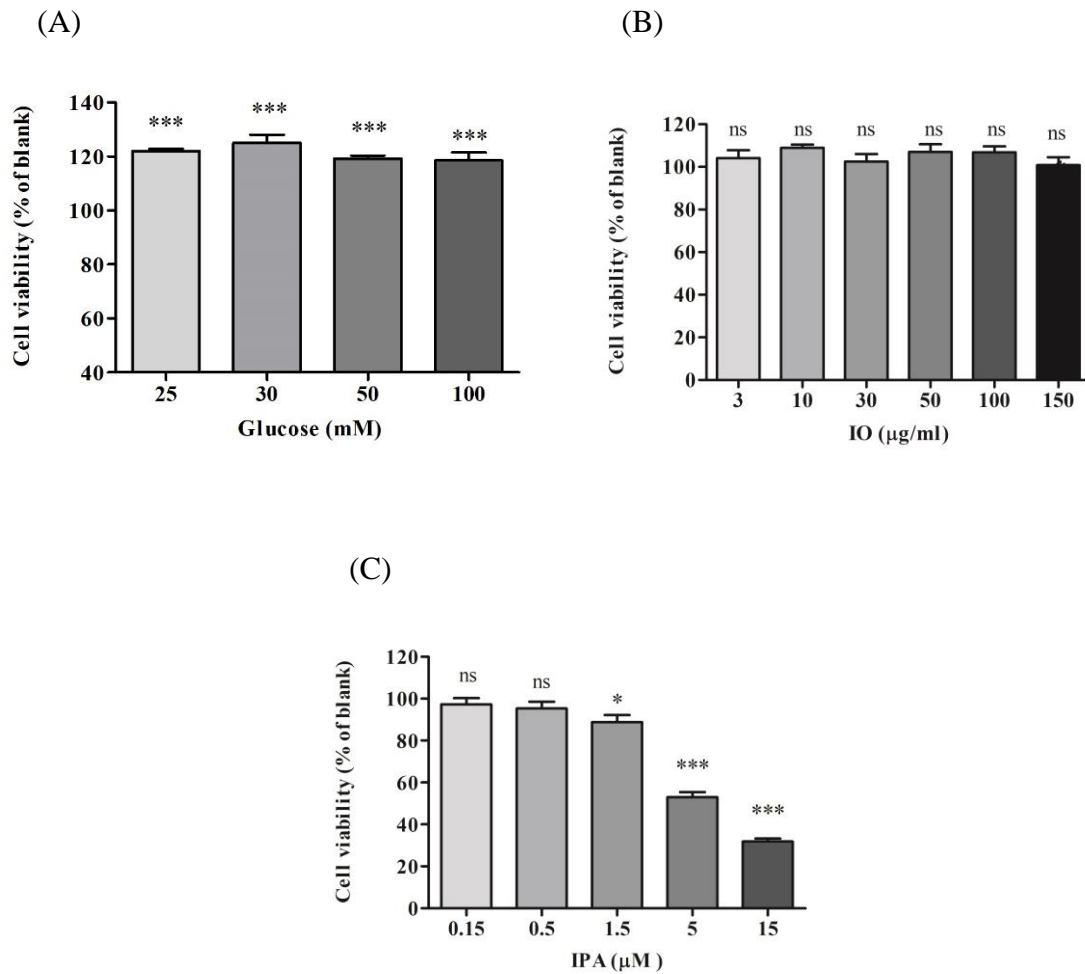


Figure 2-1. (A) HRME Cell viability upon treatment with glucose for 24 h. (B) IO cytotoxicity for HRME cells (C) IPA Cytotoxicity for HRME cells. Cells were incubated with increasing concentrations of glucose (25 mM, 30 mM, 50 mM, and 100 mM), IO extract (3 µg/ml, 10 µg/ml, 30 µg/ml, 50 µg/ml, 100 µg/ml, 150 µg/ml), IPA (0 µM, 0.15 µM, 0.5 µM, 1.5 µM, 5 µM, and 15 µM) for 24 h, and cell viability was determined by the MTT assay. Results are normalized to blank (No treatment).

2.3.2. IO extract and IPA suppress high glucose-induced cell proliferation

To evaluate whether IO extract and IPA inhibit high glucose-induced proliferation, MTT assay was performed. As shown in Figure 2-2, treatment with 30 mM of glucose increased cell viability significantly (126.0%) compared to the blank. The results show that high glucose-induced cell proliferation decreased significantly in a concentration-dependent manner with IO treatment and IPA treatment. Cell viability was found to be 11.63 %, 106.6 %, 107.7 %, 96.3 % with IO concentrations of 30 µg/ml, 50 µg/ml, 100 µg/ml, 150 µg/ml, respectively, in high glucose-treated cells. Also, Cell viability was found to be 105.6 %, 103.6 %, 98.49 %, with IPA concentrations of 0.15 µM, 0.5 µM, 1.5 µM respectively, in high glucose-treated cells. These results revealed that IO extract and IPA repressed high glucose-induced retinal endothelial cell proliferation.

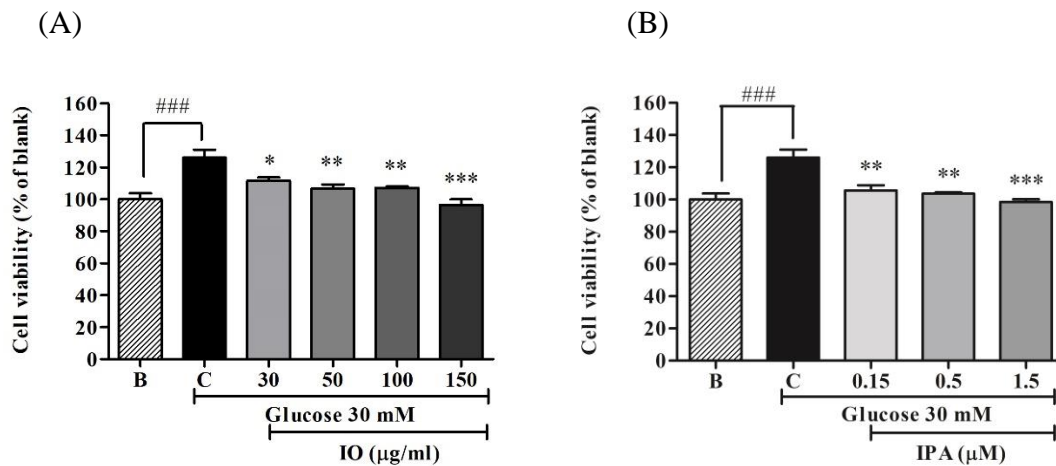
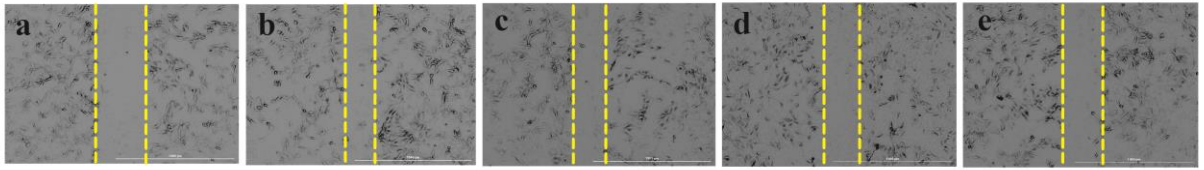


Figure 2-2. (A) Antiproliferation effect of IO extract (B). Antiproliferation effect of IPA. Cells were treated without glucose or sample (B, blank), with 30 mM of glucose without sample (C, control) and with different concentrations of IO (30 µg/ml, 50 µg/ml, 100 µg/ml, 150 µg/ml) or IPA (0.15 µM, 0.5 µM, 1.5 µM) together with 30 mM of glucose. Cells were incubated for 24 h and cell viability was measured by MTT assay. Effect of 30 mM of glucose on cell proliferation is compared with B; blank, Anti-proliferation effect of samples in high glucose-treated cells is normalized to C; control.

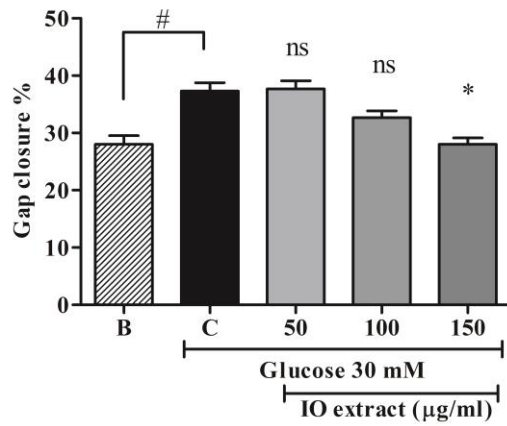
2.3.3. IO extract and IPA suppress high glucose-induced cell migration

Endothelial cell migration is one of the key steps in angiogenesis of retinopathy. To determine the influence of IO extract and IPA on the migration of retinal endothelial cells, gap closure assay was employed (Figure 2-3). Cell migration was expressed as a percentage of gap closure. Increased gap closure percentage is an indicative of higher cell migration. The results showed that treatment with 30 mM of glucose significantly increased the gap closure percentage (37.3 %), while IO extract could significantly reduce the high glucose-induced gap closure percentage in cells treated with glucose in a concentration-dependent manner. In fact, gap closure percentage was reduced to 37.3 %, 32.6 %, 28 % with IO at concentrations of 50 µg/ml, 100 µg/ml, 150 µg/ml respectively. Whereas gap closure percentage was reduced to 39.6 %, 36.2 %, 32 % with IPA at concentrations of 0.15 µM, 0.5 µM, 1.5 µM respectively. Given that gap closure is directly related to cell migration, these results suggested that IO extract and IPA inhibit the migration of retinal endothelial cells, thus contributing to its anti-angiogenic effect.

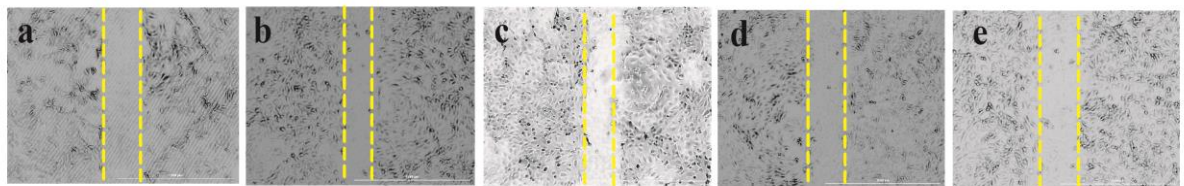
(A)



(B)



(C)



(D)

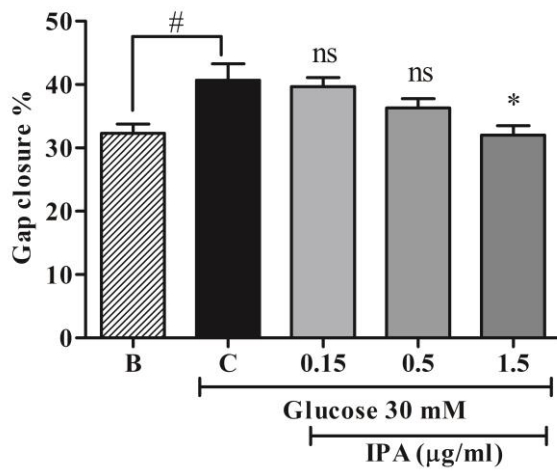
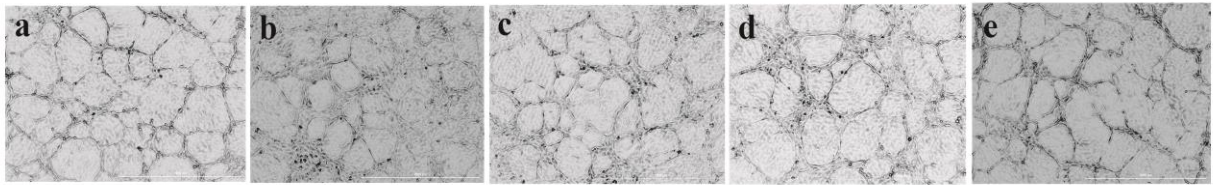


Figure 2-3. (A) IO extract inhibited the migration of EA.hy926 cells treated with high glucose concentrations. (B) Quantitative evaluation of migration inhibition of IO extract in high glucose-induced EA.hy926 cells. (C) IPA inhibited the migration of EA.hy926 cells treated with high glucose concentrations. (D) Quantitative evaluation of migration inhibition of IPA in high glucose-induced EA.hy926 cells. Cells were treated without glucose or sample (B, blank), with 30 mM of glucose without sample (C, control) and with different concentrations of IO (50 $\mu\text{g/ml}$, 100 $\mu\text{g/ml}$, 150 $\mu\text{g/ml}$) or IPA (0.15 μM , 0.5 μM , 1.5 μM) together with 30 mM of glucose.

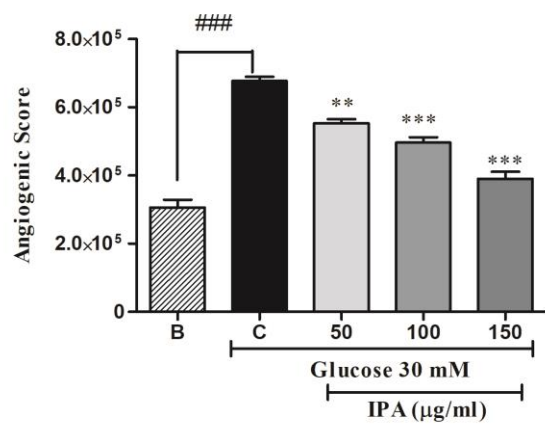
2.3.4. IO extract and IPA suppress high glucose-induced capillary formation

Tube formation/capillary-like structure formation was assessed by growing the cells on Matrigel (Figures 2-4). Angiogenic score was determined for quantitative analysis. The capillary-like tube structure network formation was significantly enhanced with 30 mM of glucose treatment, and showed an angiogenic score of 6.77×10^5 . Cells were treated together with 30 mM of glucose and different concentrations (50 $\mu\text{g/ml}$, 100 $\mu\text{g/ml}$, 150 $\mu\text{g/ml}$) of IO extract IPA in order to observe the effect of IO and IPA on high glucose-induced capillary formation. The results showed that the angiogenic score was significantly decreased to 5.52×10^5 , 4.9×10^5 , 3.9×10^5 with IO treatments of 50 $\mu\text{g/ml}$, 100 $\mu\text{g/ml}$, 150 $\mu\text{g/ml}$, respectively. With the treatment of IPA, angiogenic score was significantly decreased to 3.81×10^5 , 3.09×10^5 , 2.83×10^5 with IPA treatments of 0.15 μM , 0.5 μM , 1.5 μM , respectively. These results suggested that IO extract and IPA inhibited the capillary-like structure formation in high glucose-induced retinal endothelial cells.

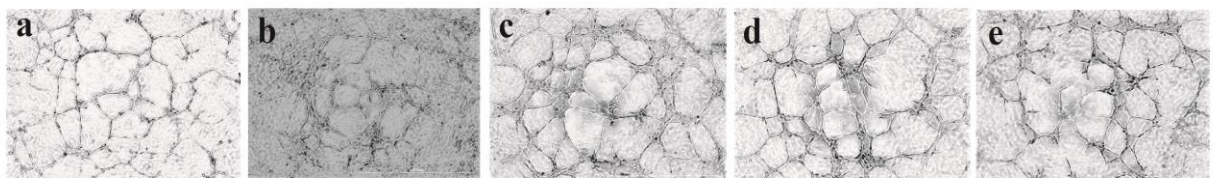
(A)



(B)



(C)



(D)

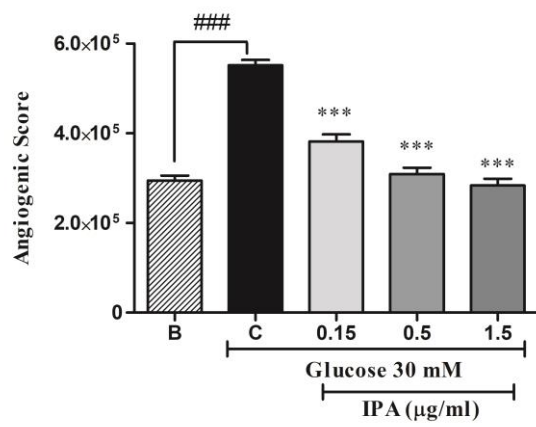


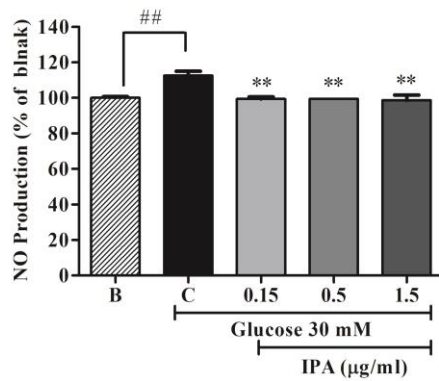
Figure 2-4. (A) IO extract inhibited the capillary formation of EA.hy926 cells treated with high glucose concentrations. (B) Quantitative evaluation of capillary formation inhibition of IO extract in high glucose-induced EA.hy926 cells. (C) IPA inhibited the capillary formation of EA.hy926 cells treated with high glucose concentrations. (D) Quantitative evaluation of capillary formation inhibition of IPA in high glucose-induced EA.hy926 cells. Cells were treated without glucose or sample (B, blank), with 30 mM of glucose without sample (C, control) and with different concentrations of IO (30 $\mu\text{g/ml}$, 50 $\mu\text{g/ml}$, 100 $\mu\text{g/ml}$, 150 $\mu\text{g/ml}$) or IPA (0.15 μM , 0.5 μM , 1.5 μM) together with 30 mM of glucose.

2.3.5. IPA inhibits NO production in high glucose treated HRME cells

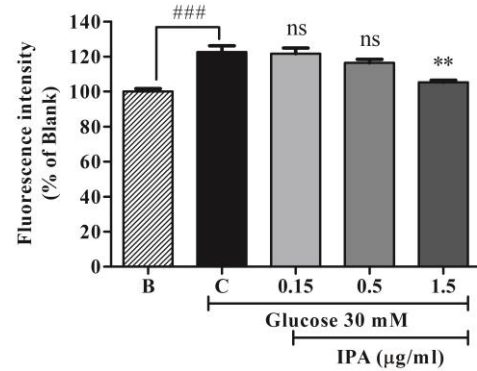
No inhibition of IPA was determined by measuring the nitrite accumulation in the cell supernatant and also using the fluorescence probe DAF FM DA. Nitrite levels in the supernatant is decreased concentration dependently (Figure 2-5A) compared to the control while fluorescence intensities exhibited the same pattern (Figure 2-5B).

In order to clear determination of NO inhibition by IPA, eNOS expression was detected in high glucose-induced HRME cells (Figure 2-5 C). As shown in figure 2-5 D, eNOS were inhibited in high glucose-induced HRME cells.

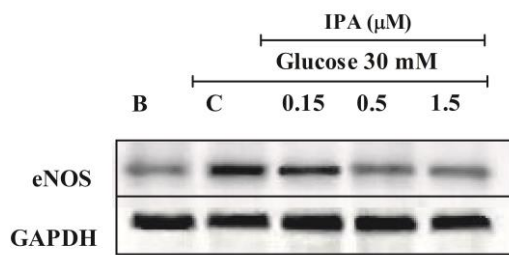
(A)



(B)



(C)



(D)

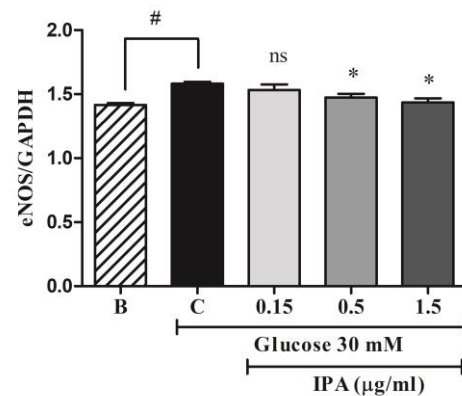


Figure 2-5. (A) IPA inhibition of NO measured by Griess assay. (B) IPA inhibition of measured by DAF FM DA assay (C) IPA inhibits eNOS (D) quantitative evaluation of NO inhibition by IPA.

2.3.6. IPA inhibits vascular permeability in vivo

Transgenic zebrafish (*flk:EGFP*) embryo were treated with CoCl_2 and tetramethylrhodamine (TAMRA) dextran. Transgenic zebrafish (*flk:EGFP*) embryo were treated with CoCl_2 to induce the vessel permeability by chemical hypoxia [10]. The vascular leakage of the permeable vessel cells were detected by treating the vessel with CoCl_2 and tetramethylrhodamine (TAMRA) dextran [11]. IPA was treated and images were taken through fluorescence microscope and fluorescence were compared (Figure 2-6B). Green bar in the graph showed vessel growth. As showed in the graph IPA suppressed the vessel growth and red color indicates the vascular leakage. With the increasing concentration of IPA vascular leakage is dramatically reduced.

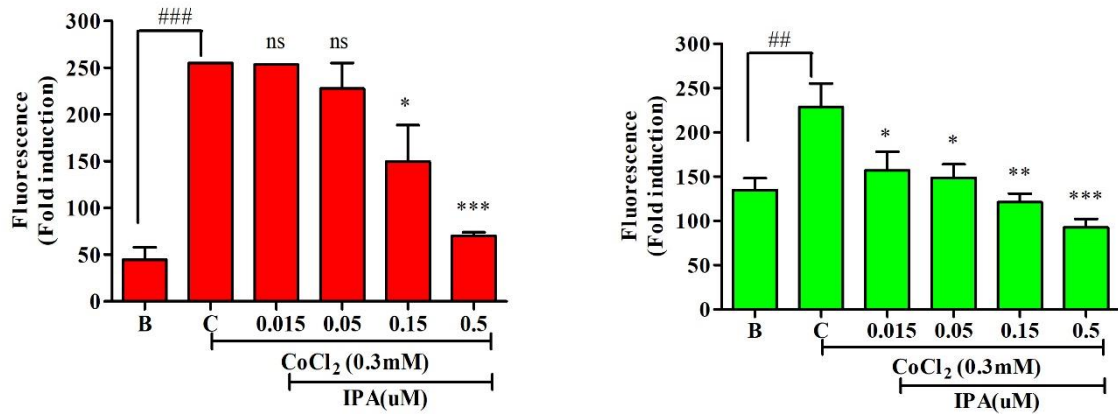
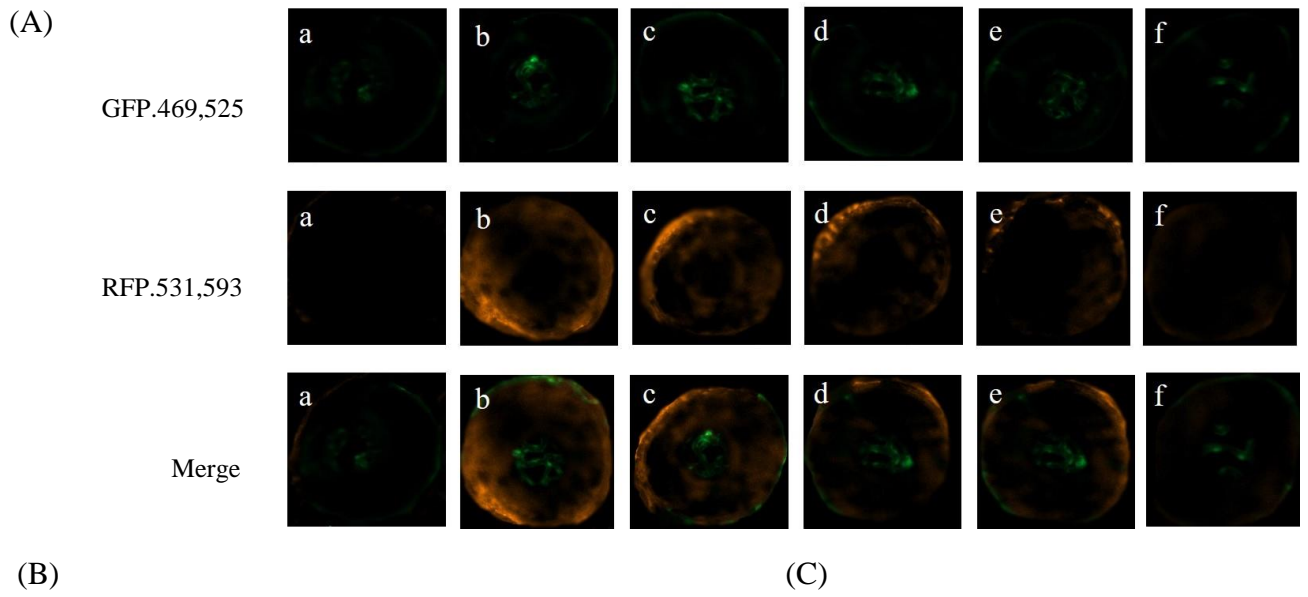


Figure 2-6. (A) IPA inhibits vascular permeability and vascular leakage in vivo. (B) Vascular leakage quantification upon the treatment of IPA against hypoxia condition (C) Quantification of vessel growth upon the treatment of IPA against hypoxia condition. (a: 0 CoCl₂ mM + 0 μM IPA, b: CoCl₂ mM + 0 μM IPA, c: CoCl₂ mM + 0.015 μM IPA, d: CoCl₂ mM + 0.05 μM IPA, e: CoCl₂ mM + 0.15 μM IPA, and f: CoCl₂ mM + 0.5 μM IPA).

2.4. Discussion

Phlorotannins are isolated from marine brown algae, and are well known for their potential as a functional ingredient in food products, pharmaceuticals, and cosmeceuticals [12]. IPA is a phlorotannin that is isolated from the marine brown alga *Ishige okamurae*. Diabetes mellitus type II is characterized by several metabolic changes, including insulin resistance, hyperinsulinemia, and hyperglycemia, which lead to vascular changes [3] and result in enhanced angiogenesis by the degradation of the extracellular matrix, and increased proliferation, survival, and migration, as well as morphological changes of endothelial cells and the development of the vascular network [13]. In the present study, the inhibitory activity of IO extract and IPA against diabetic retinopathy was evaluated.

As an initial approach, retinal vascular endothelial cells HRMEC were treated with different concentrations of glucose to mimic the angiogenesis conditions in vitro. According to the results, 30 mM of glucose treatment showed a significant increase in cell viability compared to the blank. During the retinopathy, endothelial cells undergo multiple independent processes, including detachment from basement membranes, proliferation, migration, and maturation [14].

HRME cells treated with 30 mM of glucose showed a significant induction in cell proliferation, cell migration, and capillary structure formation. IO extract and IPA showed, in a concentration-dependent manner, anti-angiogenesis activity by the significant inhibition of high glucose-induced cell proliferation, migration, and capillary structure formation in the retinal cells.

IPA inhibits NO production in high glucose-treated retinal endothelial cells indicates IPA suppress diabetic retinopathy by suppressing cell permeability. This was further confirmed by in vivo. Transgenic zebra treated with CoCl_2 and dextran showed high vascular leakage and IPA treatment suppressed the vascular leakage.

Conclusion

IO extract and IPA exhibited anti-angiogenesis effects in human retinal microvascular endothelial cells. Further studies with IPA exerted anti-angiogenesis in retinal endothelial cells by suppressing vascular permeability. This was further confirmed by suppressing vascular leakages in zebrafish embryo retina. Altogether these data suggest its use of development of therapeutics against diabetic retinopathy.

References

- 1 Volpe CMO, Villar-Delfino PH, dos Anjos PMF, Nogueira-Machado JA: Cellular death, reactive oxygen species (ROS) and diabetic complications. *Cell Death Dis* 2018;9:119.
- 2 Fong DS, Aiello L, Gardner TW, King GL, Blankenship G, Cavallerano JD, et al.: Retinopathy in Diabetes. *Diabetes Care* 2004;27:s84–s87.
- 3 Soares R: Angiogenesis in Diabetes. Unraveling the Angiogenic Paradox. *Open Circ Vasc J* 2010 [cited 2018 Apr 21];3:3–9.
- 4 Dad Bakhsh F: The Contribution Of Toll-Like Receptors In The Pathogenesis Of Diabetic Retinopathy In Human Microvascular Retinal Endothelial Cells In Vitro 2016 [cited 2019 May 24]; Available from: <https://qspace.qu.edu.qa/handle/10576/5591>
- 5 Kubes P, Granger DN: Nitric oxide modulates microvascular permeability. *Am J Physiol Circ Physiol* 1992;262:H611–H615.
- 6 Jung S-H, Kim YS, Lee Y-R, Kim JS: High glucose-induced changes in hyaloid-retinal vessels during early ocular development of zebrafish: a short-term animal model of diabetic retinopathy. *Br J Pharmacol* 2016;173:15–26.
- 7 Hansen MB, Nielsen SE, Berg K: Re-examination and further development of a precise and rapid dye method for measuring cell growth/cell kill. *J Immunol Methods* 1989;119:203–210.
- 8 Erices R, Cubillos S, Aravena R, Santoro F, Marquez M, Orellana R, et al.: Diabetic concentrations of metformin inhibit platelet-mediated ovarian cancer cell progression. *Oncotarget* 2017;8:20865–20880.
- 9 Itoh Y, Ma FH, Hoshi H, Oka M, Noda K, Ukai Y, et al.: Determination and Bioimaging Method for Nitric Oxide in Biological Specimens by Diaminofluorescein Fluorometry.

Anal Biochem 2000;287:203–209.

- 10 Wu Y-C, Chang C-Y, Kao A, Hsi B, Lee S-H, Chen Y-H, et al.: Hypoxia-Induced Retinal Neovascularization in Zebrafish Embryos: A Potential Model of Retinopathy of Prematurity. PLoS One 2015;10:e0126750.
- 11 Pink DBS, Schulte W, Parseghian MH, Zijlstra A, Lewis JD: Real-time visualization and quantitation of vascular permeability in vivo: implications for drug delivery. PLoS One 2012;7:e33760.
- 12 Li Y-X, Wijesekara I, Li Y, Kim S-K: Phlorotannins as bioactive agents from brown algae. Process Biochem 2011;46:2219–2224.
- 13 Carmeliet P, Jain RK: Angiogenesis in cancer and other diseases. Nat 2000 4076801 2000;
- 14 Pandya NM, Dhalla NS, Santani DD: Angiogenesis—a new target for future therapy. Vascul Pharmacol 2006;44:265–274.

Acknowledgement

Indeed, it gives me immense pleasure and joy to express my deepest sentiments of gratitude to everyone who not only edified but blessed me with a great deal of support and assistance in the harduous task of writing my final dissertation to culminate my two-year Master's Degree.

At first I steal a moment in this acknowledgement to express my heart-felt appreciation and gratitude to the respected Professor You-Jin Jeon for readily accepting me to the laboratory, professional guidance, support and supervision, to immerse myself in a productive research work.

I deem it indispensable at this acknowledgement to express my gratefulness to respected Dr. BoMi Ryu, for all the support, constant guidance and encouragement given me at all times. It's no exaggeration to say that without her support this research wouldn't have been a reality.

Dr. Asanka Sanjeewa is very much esteemed and appreciated for paving a path towards professor's guidance, collaboration and support throughout my research work.

At the same time my sincere gratitude goes to all the members of Marine Resource Technology lab. Special thanks goes to Hye-Won Yang, Yunfei Jiang and Jin Hwang for their support in experimental work.

It's not of second importance to express my sincere gratitude to both my dear and near ones at home for their constance love and care, encouragement and prayerful support to accomplish my research work successfully. My sincere thanks goes to my parents, brother and sister, for their love and guidance in and through all my endeavours.

Most importantly, I wish to thank my loving and supportive fiancé, Yasas Fernando, who provided me with much needed inspiration to my life.